Supported Fe/Ru catalyzed three-component relay reaction through hydrogen borrowing strategy: Conversion of crude *α*-hydroxy acids into valuable *N*-heterocycles

Shanshan Liu[a,*], Jia Wan[a], Yaoyao Zhang[a], Wen-Yu Luo[b], Weiwei Dong[a], Chao Wang[a], Lin-Yu Jiao[b,*]

[a] *Shaanxi Key Laboratory of Chemical Additives for Industry, College of Chemistry and Chemical Engineering, Shaanxi University of Science and Technology, Xi'an, Shaanxi, 710021 P. R. China*
[b] *School of Chemical Engineering, Northwest University, Xi'an, Shaanxi, 710127, P. R. China*

E-mail address:
liushanshan@sust.edu.cn (S. Liu), lyjiao@nwu.edu.cn (L.-Y. Jiao)

Table of Contents

I. Experimental Part

1.1 Materials

All reagents and reactants were procured from Energy Chemical (Shanghai) and used as received. Technical grade solvents for extraction and chromatography (ethyl acetate and petroleum ether) were distilled prior to use and other solvents were used directly without further purification.

1.2 Instrumentation Methods

The X-ray diffraction (XRD) patterns were obtained by a powder X-ray diffractometer (SmartLAB SE, Rigaku). Scanning electron microscope (SEM) and transmission electron microscopy (TEM) were used to study the size and morphology of the materials. SEM was performed on the Zeiss Gemini SEM 360 instrument and TEM was performed on the FEI-TALOS-F200X instrument. The X-ray photoelectron spectroscopy (XPS) was conducted with a Thermo Fisher Scientific Nexsa™ instrument equipped with an Al Kα X-ray radiation source (*hv* = 1486.6 eV). Analytical thin layer chromatography (TLC) was performed on silica gel GF254 glass plates from Qingdao Haiyang Chemical Co. Lt. Flash column chromatography was performed on silica gel (300–400 mesh) by Qingdao Haiyang Chemical Co. Lt using the indicated solvents. ^{1}H and ^{13}C NMR spectra were recorded in $CDCl_3$ on Bruker Avance III 400 MHz instrument. Chemical shifts are reported in parts per million (ppm) downfield from tetramethylsilane (TMS) and are referenced to the residual solvent resonance as the internal standard ($CHCl_3$: δ = 7.26 ppm for ^{1}H and $CDCl_3$: δ = 77.16 ppm for ^{13}C). Data are reported as follows: chemical shift, multiplicity (br s = broad singlet, s = singlet, d = doublet, t = triplet, q = quartet, m = multiplet), coupling constants (Hz) and integration. High performance liquid chromatography (HPLC) was detected on the Shimidazu LC-20AD with a photodiode detector (Shimadzu SPD-M20A), mobile phase: acetonitrile/water = 70/30 (*v*/*v*); wavelength: 259 nm; flow rate: 1.0 mL/min. The gas phase pf the reaction mixture was analyzed by gas chromatography (GC-7820) using a TDX-01 column on a thermal conductivity detector (TCD) with a Plot-Q column on a hydrogen flame ionization detector (FID). NH_3 temperature programmed desorption (NH_3-TPD) was carried out on a MicrotracBEL BelCata II chemisorption analyzer. 100 mg sample loaded in a quartz reactor was pretreated with Ar at 500 °C. After cooling to 50 °C, NH_3 adsorption was performed by switching Ar to NH_3 gas and then maintaining 2 h. After adsorption, the physical adsorption of

NH_3 was removed at the same temperature by Ar purging for 1 h. Then, TPD was detected by Thermal Conductive Detector (TCD) in the Ar flow by raising the temperature to 500 °C at a rate of 10 °C/min.

1.3 Preparation of Catalyst Fe-Ru/*γ*-Al_2O_3

Initially, *γ*-Al_2O_3 (546 mg) was added to an aqueous solution of $Fe(NO_3)_3 \cdot 9H_2O$ (0.81 mmol, 325 mg), and the resulting mixture was evaporated slowly until dryness at 65 °C overnight. Then, nitrates were removed with the solid sample being kept at 280 °C for 4 h under a N_2 atmosphere. Afterwards, the *γ*-Al_2O_3 supported Fe material was obtained through a reduction process with H_2 at 300 °C for 3 h. Subsequently, Ru particle was anchored on the *γ*-Al_2O_3 by using the same method with $RuCl_3 \cdot 3H_2O$ (0.50 mmol, 130 mg) as precursor. The resulting material was desired catalyst and denoted as Fe-Ru/*γ*-Al_2O_3.

II. Reaction Results

2.1 General Procedure for the Catalysis

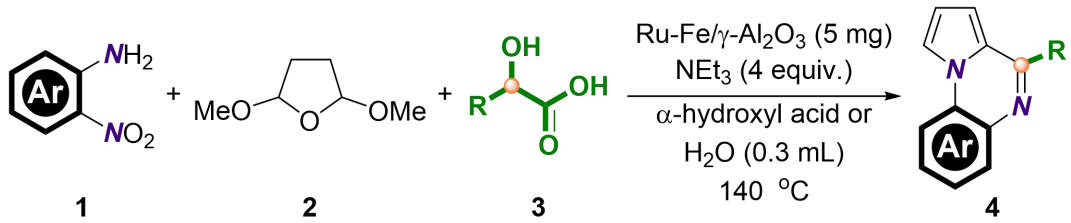

1 **2** **3** **4**

General procedure (**GP**): The pressure tube was filled with 2-nitro aromatic amine (**1**, 0.10 mmol), 2,5-dimethoxytetrahydrofuran (**2**, 0.15 mmol) and *α*-hydroxy acid (**3**, 0.30 mL; for other *α*-hydroxy acids, 5.0 equiv. was used in the combination of 0.3 mL H_2O as solvent), Et_3N (4.0 equiv.) and Fe-Ru/*γ*-Al_2O_3 (5.0 mg) as heterogeneous catalyst. The reaction mixture was stirred at 140 °C under air for 6 h. After cooling to room temperature, the mixture was removed under reduced pressure. The residue was purified by flash silica gel chromatography to afford the desired analytical pure product **4**.

2.2 Characterization of the Products

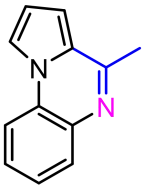

4-Methylpyrrolo[1,2-*a*]quinoxaline (4aa)

Pale yellow solid (14.0 mg, 77% yield). Petroleum ether/ethyl acetate = 30:1, R_f = 0.30. ^{1}H NMR (400 MHz, $CDCl_3$): *δ* = 7.96 – 7.88 (m, 2H), 7.83 (d, *J* = 7.9 Hz, 1H), 7.53 – 7.40 (m, 2H), 6.93 – 6.84 (m, 2H), 2.76 (s, 3H) ppm. ^{13}C NMR (101 MHz, $CDCl_3$): *δ* = 153.5, 135.9, 129.3, 127.3, 126.9, 126.3, 125.1, 114.2, 113.7, 113.5, 106.5, 22.0 ppm.

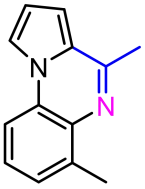

4,6-Dimethylpyrrolo[1,2-*a*]quinoxaline (4ba)

Pale yellow solid (14.2 mg, 72% yield). Petroleum ether/ethyl acetate = 30:1, R_f = 0.35. ^{1}H NMR (400 MHz, $CDCl_3$): *δ* = 8.33 (dd, *J* = 2.9 Hz, 1.4 Hz, 1H), 7.83 (dd, *J* = 7.7 Hz,

1.9 Hz, 1H), 7.37 – 7.28 (m, 2H), 6.96 (dd, *J* = 4.0 Hz, 1.4 Hz, 1H), 6.87 (dd, *J* = 4.1 Hz, 2.8 Hz, 1H), 2.97 (s, 3H), 2.76 (s, 3H) ppm. ^{13}C NMR (101 MHz, $CDCl_3$): *δ* = 153.3, 137.5, 130.5, 127.7, 125.4, 125.4,124.6, 120.0, 112.9, 106.1, 24.0, 21.9 ppm.

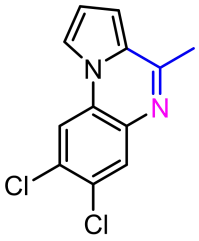

7,8-Dichloro-4-methylpyrrolo[1,2-*a*]quinoxaline (4ca)

Pale yellow solid (16.3 mg, 65% yield). Petroleum ether/ethyl acetate = 20:1, R_f = 0.38. ^{1}H NMR (400 MHz, $CDCl_3$): *δ* = 7.96 (s, 1H), 7.88 (s, 1H), 7.81 (dd, *J* = 2.8 Hz, 1.4 Hz, 1H), 6.94 (dd, *J* = 4.1 Hz, 1.3 Hz, 1H), 6.89 (dd, *J* = 4.1 Hz, 2.8 Hz, 1H), 2.72 (s, 3H) ppm. ^{13}C NMR (101 MHz, $CDCl_3$): *δ* = 155.2, 135.4, 130.3 (d, *J* = 11.2 Hz),130.2, 128.6, 126.5, 126.0, 115.3, 114.8, 114.4, 107.7, 22.1 ppm.

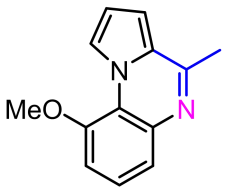

9-Methoxy-4-methylpyrrolo[1,2-*a*]quinoxaline (4da)

Pale yellow solid (14.8 mg, 70% yield). Petroleum ether/ethyl acetate = 5:1, R_f = 0.35. ^{1}H NMR (400 MHz, $CDCl_3$): *δ* = 8.75 (dd, *J* = 2.9 Hz, 1.4 Hz, 1H), 7.60 – 7.53 (m, 1H), 7.37 (t, *J* = 8.2 Hz, 1H), 7.05 (d, *J* = 8.1 Hz, 1H), 6.95 (dd, *J* = 4.1 Hz, 1.4 Hz, 1H), 6.86 – 6.80 (m, 1H), 4.10 (s, 3H), 2.76 (s, 3H) ppm. ^{13}C NMR (101 MHz, $CDCl_3$): *δ* = 153.9, 149.8, 138.2, 126.8, 124.3, 122.1, 121.3, 118.7, 112.5, 108.5, 105.9, 56.2, 22.0 ppm.

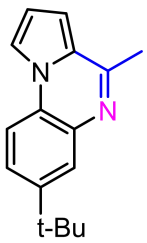

7-(*tert*-Butyl)-4-methylpyrrolo[1,2-*a*]quinoxaline (4ea)

Yellow oil (11.6 mg, 50% yield). Petroleum ether/ethyl acetate = 30:1, R_f = 0.35. ^{1}H NMR (400 MHz, $CDCl_3$): *δ* = 7.85 (dd, *J* = 4.2 Hz, 2.1 Hz, 1H), 7.79 (q, *J* = 5.5 Hz, 4.3

Hz, 1H), 7.71 – 7.63 (m, 1H), 7.45 (ddd, *J* = 8.7 Hz, 4.1 Hz, 2.1 Hz, 1H), 6.82 – 6.70 (m, 2H), 2.65 (s, 3H), 1.33 (s, 9H) ppm. ^{13}C NMR (101 MHz, $CDCl_3$): *δ* = 153.6, 148.4, 135.6, 126.3, 125.7, 125.1, 124.6, 114.1, 113.3, 113.2, 106.3, 34.8, 31.5, 22.1 ppm.

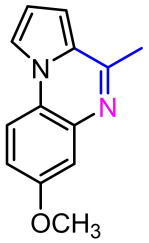

7-Methoxy-4-methylpyrrolo[1,2-*a*]quinoxaline (4fa)

Pale yellow solid (15.3 mg, 72% yield). Petroleum ether/ethyl acetate = 5:1, R_f = 0.40. ^{1}H NMR (400 MHz, $CDCl_3$): *δ* = 7.84 (s, 1H), 7.75 (d, *J* = 9.0 Hz, 1H), 7.41 (d, *J* = 2.8 Hz, 1H), 7.11 (dd, *J* = 9.0 Hz, 2.8 Hz, 1H), 6.90 (dd, *J* = 3.9 Hz, 1.4 Hz, 1H), 6.84 (dd, *J* = 4.0 Hz, 2.6 Hz, 1H), 3.94 (s, 3H), 2.75 (s, 3H) ppm. ^{13}C NMR (101 MHz, $CDCl_3$): *δ* = 157.1, 154.1, 137.0, 126.0, 121.6, 116.0, 114.6, 114.0, 113.2, 110.6, 106.3, 55.7, 22.1 ppm.

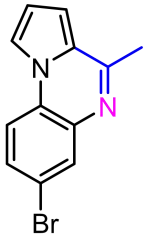

7-Bromo-4-methylpyrrolo[1,2-*a*]quinoxaline (4ga)

Pale yellow solid (15.5 mg, 60% yield). Petroleum ether/ethyl acetate = 20:1, R_f = 0.33. ^{1}H NMR (400 MHz, $CDCl_3$): *δ* = 8.07 (d, *J* = 2.2 Hz, 1H), 7.89 (dd, *J* = 2.8 Hz, 1.4 Hz, 1H), 7.71 (d, *J* = 8.8 Hz, 1H), 7.58 (dd, *J* = 8.7 Hz, 2.2 Hz, 1H), 6.94 (dd, *J* = 4.0 Hz, 1.4 Hz, 2H), 2.75 (s, 3H) ppm. ^{13}C NMR (101 MHz, $CDCl_3$): *δ* = 155.0, 137.2, 131.8, 129.7, 126.4, 126.3, 117.7, 115.1, 114.6, 114.0, 107.2, 22.1 ppm.

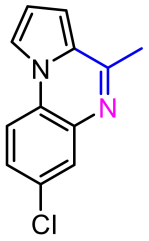

7-Chloro-4-methylpyrrolo[1,2-*a*]quinoxaline (4ha)

White solid (13.9 mg, 65% yield). Petroleum ether/ethyl acetate = 20:1, R_f = 0.28. ^{1}H

NMR (400 MHz, $CDCl_3$): δ = 7.92 – 7.86 (m, 2H), 7.80 (d, J = 8.7 Hz, 1H), 7.47 (dd, J = 8.8 Hz, 2.3 Hz, 1H), 6.93 (dt, J = 21.2 Hz, 3.4 Hz, 2H), 2.77 (s, 3H) ppm. ^{13}C NMR (101 MHz, $CDCl_3$): δ = 154.9, 136.9, 130.2, 128.7, 126.9, 126.1, 125.9, 114.7, 114.5, 113.9, 107.1, 22.0 ppm.

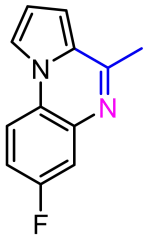

7-Fluoro-4-methylpyrrolo[1,2-*a*]quinoxaline (4ia)

White solid (13.2 mg, 66% yield). Petroleum ether/ethyl acetate = 20:1, R_f = 0.30. ^{1}H NMR (400 MHz, $CDCl_3$): δ = 7.96 – 7.86 (m, 1H), 7.82 (dd, J = 9.0 Hz, 5.1 Hz, 1H), 7.64 (ddd, J = 23.1 Hz, 9.5 Hz, 2.8 Hz, 1H), 7.31 – 7.20 (m, 1H), 6.99 – 6.86 (m, 2H), 2.76 (s, 3H) ppm. ^{13}C NMR (101 MHz, $CDCl_3$): δ = 159.8 (d, J = 241.8 Hz), 154.9, 137.1 (d, J = 11.3 Hz), 126.0, 123.9, 114.7 (d, J = 4.6 Hz), 114.6, 114.5, 114.4, 113.6, 106.9, 22.0 ppm.

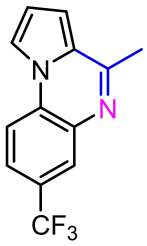

4-Methyl-7-(trifluoromethyl)pyrrolo[1,2-*a*]quinoxaline (4ja)

White solid (17.3 mg, 69% yield). Petroleum ether/ethyl acetate = 20:1, R_f = 0.37. ^{1}H NMR (400 MHz, $CDCl_3$): δ = 8.20 (s, 1H), 7.97 – 7.87 (m, 2H), 7.71 (dd, J = 8.5 Hz, 2.1 Hz, 1H), 7.00 – 6.90 (m, 2H), 2.77 (s, 3H) ppm. ^{13}C NMR (101 MHz, $CDCl_3$): δ = 155.3, 135.6, 129.4, 127.4, 126.9, 126.4, 123.4, 122.7, 115.0, 114.5, 114.3, 107.6, 22.1 ppm. ^{19}F NMR (376 MHz, $CDCl_3$): δ = -61.9 ppm. HRMS (ESI) m/z calculated for $C_{13}H_9F_3N_2$ $[M+H]^+$: 251.0791, found: 251.0795.

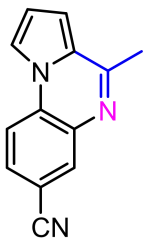

4-Methylpyrrolo[1,2-*a*]quinoxaline-7-carbonitrile (4ka)

Pale yellow solid (10.3 mg, 50% yield). Petroleum ether/ethyl acetate = 5:1, R_f = 0.35. ^{1}H NMR (400 MHz, $CDCl_3$): δ = 8.21 (s, 1H), 7.96 (d, J = 2.8 Hz, 1H), 7.91 (d, J = 8.5 Hz, 1H), 7.73 (dd, J = 8.3 Hz, 1.9 Hz, 1H), 7.04 – 6.95 (m, 2H), 2.77 (s, 3H) ppm. ^{13}C NMR (101 MHz, $CDCl_3$): δ = 155.9, 135.9, 133.9, 130.3, 129.7, 126.4, 118.6, 115.3, 115.1, 114.9, 108.5, 108.2, 22.1 ppm.

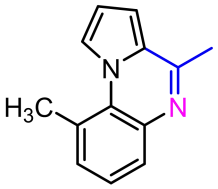

4,9-Dimethylpyrrolo[1,2-*a*]quinoxaline (4la)

Pale yellow solid (13.9 mg, 71% yield). ^{1}H NMR (400 MHz, $CDCl_3$): δ = 8.30 (d, J = 2.7 Hz, 1H), 7.83 (d, J = 7.9 Hz, 1H), 7.32 (dt, J = 15.7 Hz, 7.6 Hz, 2H), 6.94 (d, J = 3.8 Hz, 1H), 6.88 – 6.84 (m, 1H), 2.95 (s, 3H), 2.75 (s, 3H) ppm. ^{13}C NMR (101 MHz, $CDCl_3$): δ = 153.2, 137.5, 130.5, 127.7, 127.6, 127.5, 125.3, 124.5, 119.9, 112.8, 106.0, 23.9, 21.9 ppm.

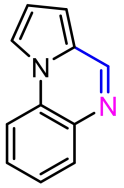

Pyrrolo[1,2-*a*]quinoxaline (4ab)

Pale yellow solid (10.7 mg, 64% yield). ^{1}H NMR (400 MHz, $CDCl_3$): δ = 8.82 (s, 1H), 7.98 (dd, J = 8.1 Hz, 1.5 Hz, 1H), 7.93 – 7.89 (m, 1H), 7.84 (dd, J = 8.1 Hz, 1.4 Hz, 1H), 7.63 – 7.41 (m, 2H), 6.90 (dd, J = 10.0 Hz, 3.4 Hz, 2H) ppm. ^{13}C NMR (101 MHz, $CDCl_3$): δ = 145.7, 135.7, 130.0, 127.8, 126.4, 125.2, 114.3, 114.1, 113.8, 110.1, 107.5 ppm.

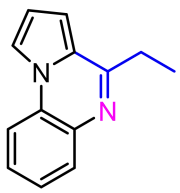

4-Ethylpyrrolo[1,2-*a*]quinoxaline (4ac)

Yellow solid (13.8 mg, 71% yield). Petroleum ether/ethyl acetate = 30:1, R_f = 0.30. ^{1}H

NMR (400 MHz, $CDCl_3$): δ = 8.02 – 7.94 (m, 2H), 7.88 (dd, J = 8.1 Hz, 1.6 Hz, 1H), 7.56 – 7.43 (m, 2H), 6.97 (d, J = 3.9 Hz, 1H), 6.90 (t, J = 3.3 Hz, 1H), 3.11 (q, J = 7.6 Hz, 2H), 1.50 (t, J = 7.6 Hz, 3H) ppm. ^{13}C NMR (101 MHz, $CDCl_3$): δ = 158.5, 136.1, 129.3, 127.0, 126.9, 125.2, 125.0, 114.4, 113.7 (d, J = 7.4 Hz), 113.4, 106.1, 29.0, 12.8 ppm. HRMS (ESI) m/z calculated for $C_{13}H_{12}N_2$ $[M+H]^+$: 197.1073, found: 197.1071.

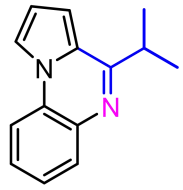

4-(1-Methylethyl)pyrrolo[1,2-*a*]quinoxaline (4ad)

Pale yellow solid (9.3 mg, 45% yield). Petroleum ether/ethyl acetate = 30:1, R_f = 0.35. ^{1}H NMR (400 MHz, $CDCl_3$): δ = 7.99 (d, J = 7.8 Hz, 2H), 7.87 (dd, J = 7.9 Hz, 1.6 Hz, 1H), 7.48 (dtd, J = 19.3 Hz, 7.4 Hz, 1.5 Hz, 2H), 6.97 (d, J = 3.9 Hz, 1H), 6.92 – 6.86 (m, 1H), 3.64 – 3.32 (m, 1H), 1.50 (d, J = 6.9 Hz, 6H) ppm. ^{13}C NMR (101 MHz, $CDCl_3$): δ = 161.8, 129.7, 127.3, 125.5, 125.2, 125.0, 115.1, 112.1,113.6, 113.3, 105.9, 33.3, 29.8, 21.1 ppm.

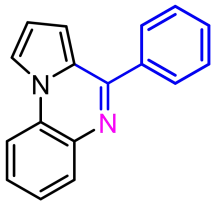

4-Phenylpyrrolo[1,2-*a*]quinoxaline (4ae)

Pale yellow solid (15.8 mg, 65% yield). Petroleum ether/ethyl acetate = 30:1, R_f = 0.35. ^{1}H NMR (400 MHz, $CDCl_3$): δ = 8.13 – 8.01 (m, 4H), 7.93 (d, J = 8.1 Hz, 1H), 7.65 – 7.42 (m, 5H), 7.05 (d, J = 4.0 Hz,1H), 6.95 (t, J = 3.3 Hz, 1H) ppm. ^{13}C NMR (101 MHz, $CDCl_3$): δ = 154.5, 138.4, 136.2, 130.1, 129.9, 128.7, 128.7,127.6, 127.2, 125.4, 125.3, 114.8, 114.1, 113.7, 109.0 ppm.

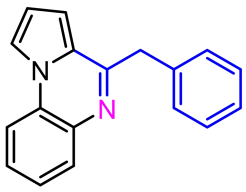

4-(Phenylmethyl)pyrrolo[1,2-*a*]quinoxaline (4af)

Pale yellow solid (15.0 mg, 58% yield). ^{1}H NMR (400 MHz, $CDCl_3$): δ = 8.12 (d, J = 8.1 Hz, 1H), 8.08 – 8.02 (m, 3H), 7.94 (d, J = 8.2 Hz, 1H), 7.62 – 7.57 (m, 4H), 7.57 – 7.47 (m, 1H), 7.06 (d, J = 3.9 Hz, 1H), 6.96 (t, J = 3.3 Hz, 1H), 1.31 (d, J = 10.2 Hz, 2H) ppm. ^{13}C NMR (101 MHz, $CDCl_3$): δ = 130.1 (d, J = 24.6 Hz), 128.7 (d, J = 3.3 Hz), 127.6, 127.2, 125.4, 114.5 (d, J = 68.3 Hz), 113.7 ppm.

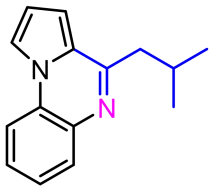

4-(2-Methylpropyl)pyrrolo[1,2-*a*]quinoxaline (4ag)

Yellow oil (11.7 mg, 52% yield). ^{1}H NMR (400 MHz, $CDCl_3$): δ = 7.94 (d, J = 7.9 Hz, 1H), 7.88 (s, 1H),7.80 (d, J = 7.8 Hz, 1H), 7.43 (p, J = 7.2 Hz, 2H), 6.89 (d, J = 4.0 Hz, 1H), 6.83 (q, J = 2.9 Hz, 1H), 2.89 (dd, J = 7.3 Hz, 2.2 Hz, 2H), 2.42 – 2.40 (m, 1H), 1.04 (dd, J = 6.6 Hz, 2.3 Hz, 6H) ppm. ^{13}C NMR (101 MHz, $CDCl_3$): δ = 156.9, 136.2, 129.7, 127.4, 126.9, 126.8, 125.1, 114.1, 113.7, 113.5, 106.5, 44.8, 28.5, 23.0 ppm.

2.3 Scaled Up Reaction and Catalyst Reusability

The pressure tube was filled with 2-nitro aniline (**1a**, 1.0 mmol), 2,5-dimethoxytetrahydrofuran (**2**, 1.5 equiv.), lactic acid (**3a**, 3 mL), Et_3N (4.0 equiv.), and anhydrous Fe-Ru/γ-Al_2O_3 (50 mg) as heterogeneous catalyst. The reaction mixture was stirred at 140 °C under air for 12 h. After cooling to room temperature, the catalyst was recovered by centrifugation and further subjected to the subsequent reaction, which can be conducted smoothly and did not need to add nothing but new substrates. The liquid system was removed under reduced pressure, and the residue was purified by flash silica gel chromatography to afford the desired analytical pure product **4aa** (123 mg, 68%, 120 mg, 66%, 122 mg, 67%, 118 mg, 65%, and 114.6 mg, 63% in five runs, respectively).

2.4 Leaching Test

In order to clarify if leached species, such as metal ions, has contributed to the formation of **4aa**, a hot-filtration experiment was conducted. With the addition of 2-nitro aniline (**1a**, 0.10 mmol), 2,5-dimethoxytetrahydrofuran (**2**, 0.15 mmol), lactic acid (**3a**, 0.3 mL), and Et_3N (4.**0** equiv.) successively, the system has been filtrated after proceeding at 140 °C for 5 min. Subsequently, the mixture was allowed to

conduct under standard conditions in the absence of the catalyst. To our expect, only 2% of **4aa** was detected after 6 h, indicating the stability of the supported catalyst and the reaction proceeding in a heterogeneous catalytic fashion.

III. Synthetic Utility

3.1 Catalytic Transformation from Glucose

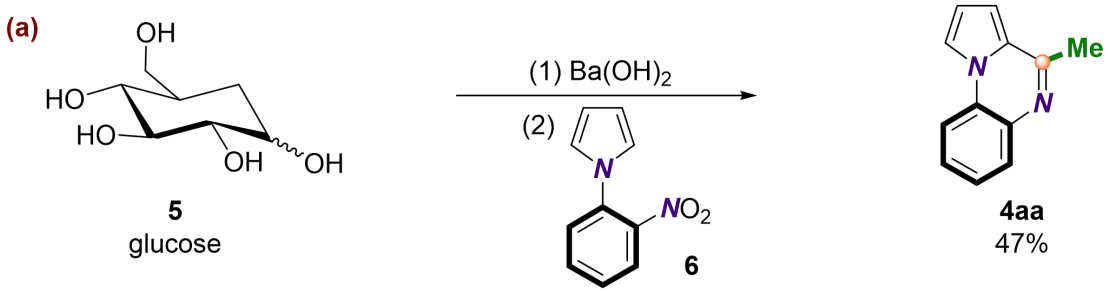

To a pressure tube containing a magnetic stirrer were added glucose (**5**, 0.5 mmol), $Ba(OH)_2$ (1.5 mmol), and H_2O (5.0 mL) at room temperature under nitrogen atmosphere. After 48 h, (2-nitrophenyl)-1*H*-pyrrole (**6**, 0.10 mmol) and Fe-Ru/*γ*-Al_2O_3 (5.0 mg) were added into the mixture for additional 12 h. Afterwards, the mixture was removed under reduced pressure and the residue was purified by silica gel chromatography to afford the product **4aa** in 47% yield.

3.2 Catalytic Transformation from Fruits

mixed acids

Fruit	Distribution of mixed acids (100% total)		
	Malic acid (%)	Citric acid (%)	Tartric acid (%)
Apple	96.3	2.3	1.4
Orange	8.1	91.9	0
Grape	38.7	4.3	57.0

Scheme S1. Procedure of the catalytic transformation from fruits and the mixed acids distribution of the fruits' extraction

By weight, take 100 parts of fruit pulp (apple, orange, or grape), add 180 parts of water and 8 parts of cellulase, perform enzymatic hydrolysis (at 55 °C for 2 h), inactivate enzymes, and obtain enzymatic hydrolysate. The system was filtered and the filtrate was concentrated to reduce the volume by approximately half, followed by the addition of an equal volume of ethanol aqueous solution (EtOH:H_2O = 1:1). The organic phase was separated and an equal volume of 1.5 wt% of sodium hydroxide

aqueous solution was added subsequently. After stirring for 20 min, the aqueous phase was collected and treated with an ultrafiltration membrane (50000–100000 Daltons) for filtration. The resulting filtrate was concentrated under reduced pressure, decolorization with activated carbon, recrystallization and washed with ethyl acetate to provide the mixed acids as solid, with main ingredients of malic acid, citric acid, and tartaric acid (Scheme S1, Figures S1–S3, and Tables S1–S3).

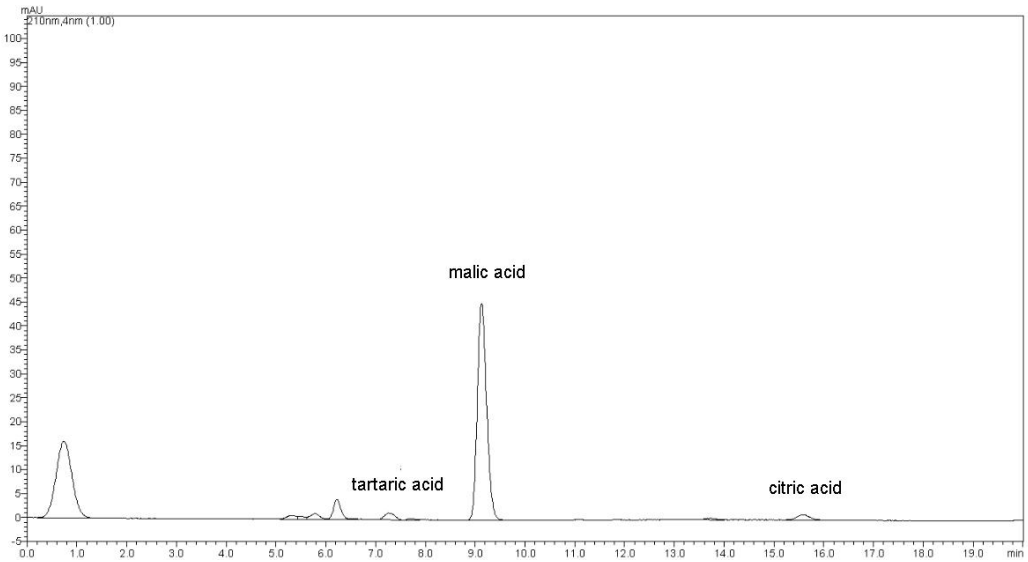

Figure S1. Mixed acids from apple

Table S1. HPLC analysis results

Substance	Retention time	Area	Ratio (%)
tartaric acid	7.259	8326	1.4
malic acid	9.123	586851	96.3
citric acid	15.588	14034	2.3

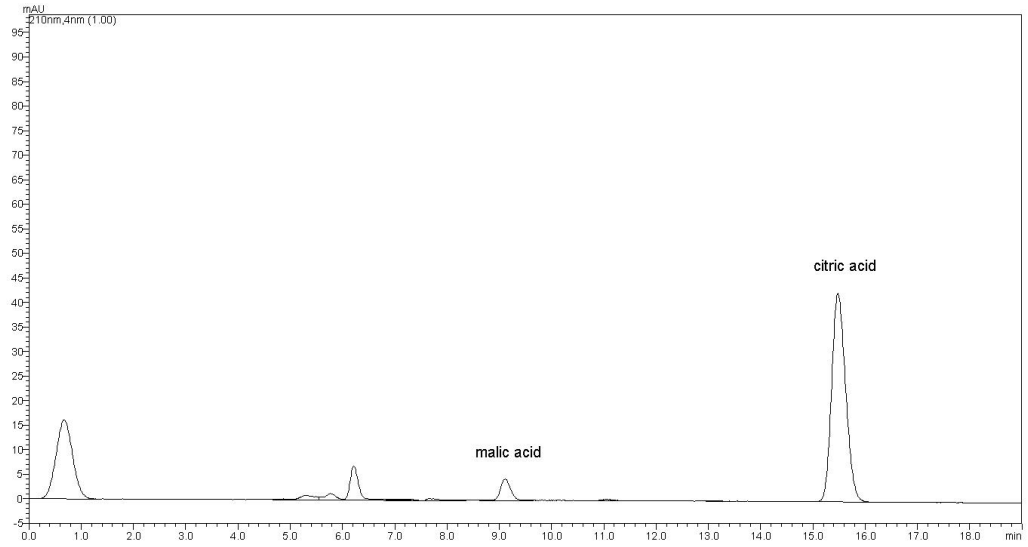

Figure S2. Mixed acids from orange

Table S2. HPLC analysis results

Substance	Retention time	Area	Ratio (%)
tartaric acid	-	-	0
malic acid	9.109	70082	8.1
citric acid	15.472	790112	91.9

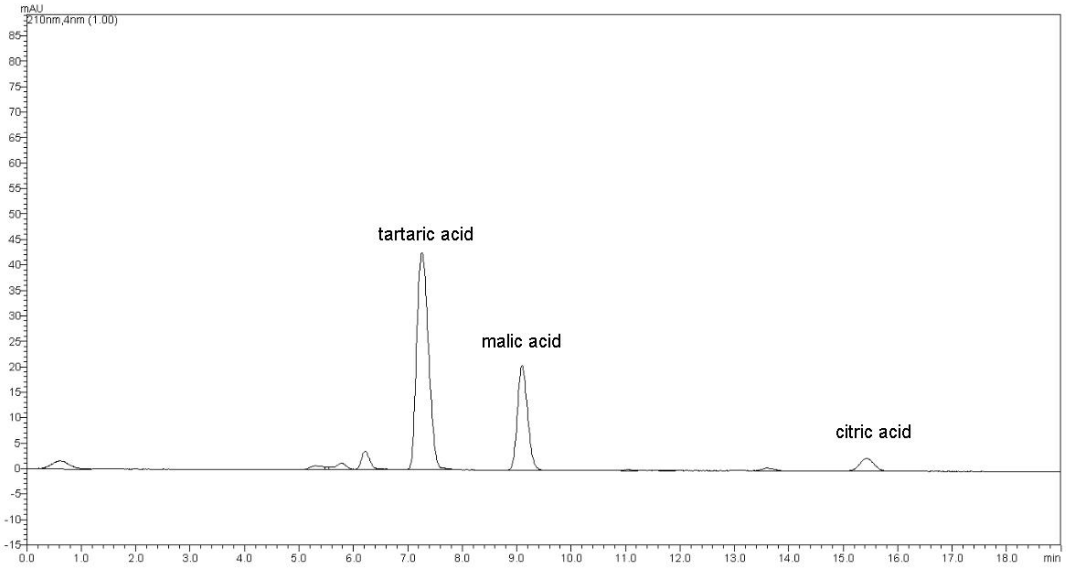

Figure S3. Mixed acids from grape

Table S3. HPLC analysis results

Substance	Retention time	Area	Ratio (%)
tartaric acid	7.253	542198	57.0
malic acid	9.094	368798	38.7
citric acid	15.421	40978	4.3

Table S4 Catalytic transformation of mixed acids and model substrate

Acids	Yield of 4ab[a]
Mixed acids from apple	69% (43%[b])
Mixed acids from orange	23% (traces[b])
Mixed acids from grape	48% (28%[b])
malic acid	84% (61%[b])
citric acid	42% (n.d.[b])
tartric acid	67% (34%[b])

[a]**6** was used as substrate. [b]**1a** and **2** were used as substrates.

The mixed acids (0.5 mmol) from apple, orange or grape were subjected to **6** under Fe-Ru/γ-Al_2O_3 (5.0 mg), Et_3N (0.4 mmol), H_2O (0.3 mL), **4ab** was obtained in 69%, 23%, and 48% yield, respectively. Moreover, The mixed acids (0.5 mmol) from fruits were subject to **1a** (0.10 mmol), **2** (0.15 mmol) under standard conditions to give **4ab** in 43% yield refer to mixed acids from apple, 28% yield refer to that from grape, while traces amount of product was observed refer to that from orange, respectively. The result were shown above in Table S4.

The α-hydroxy acid such as malic acid, citric acid, and tartric acid (0.5 mmol) was subject to **6** under Fe-Ru/γ-Al_2O_3 (5.0 mg), Et_3N (0.4 mmol), H_2O (0.3 mL), **4ab** was obtained in 84%, 42%, and 67% yield, respectively (Table S4). When it was added into **1a** (0.10 mmol), **2** (0.15 mmol) under standard conditions, **4ab** was obtained in 61% yield refer to malic acids, 34% yield refer to tartric acid, while no product was observed when citric acid was used.

3.3 Plausible Pathway for the Conversion of Mixed Acids

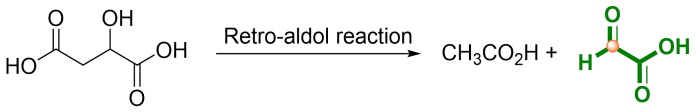

Scheme S2. Possible reaction pathway for the conversion of malic acid

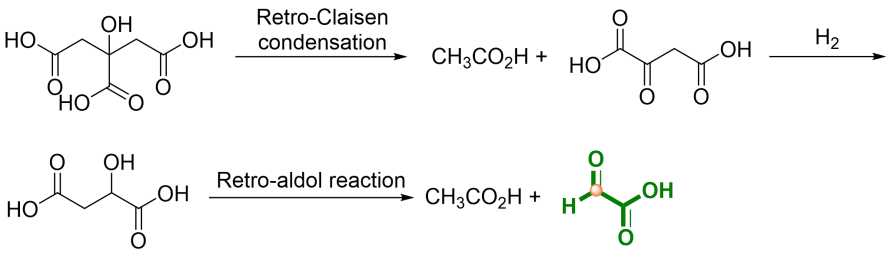

Scheme S3. Possible reaction pathway for the conversion of citric acid

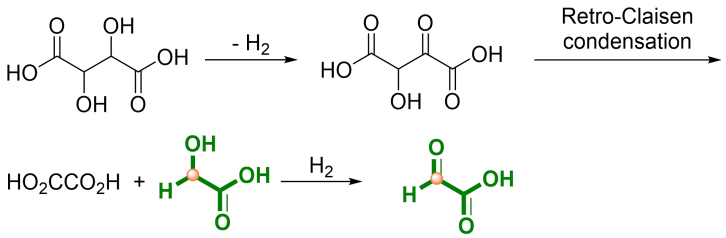

Scheme S4. Possible reaction pathway for the conversion of tartaric acid

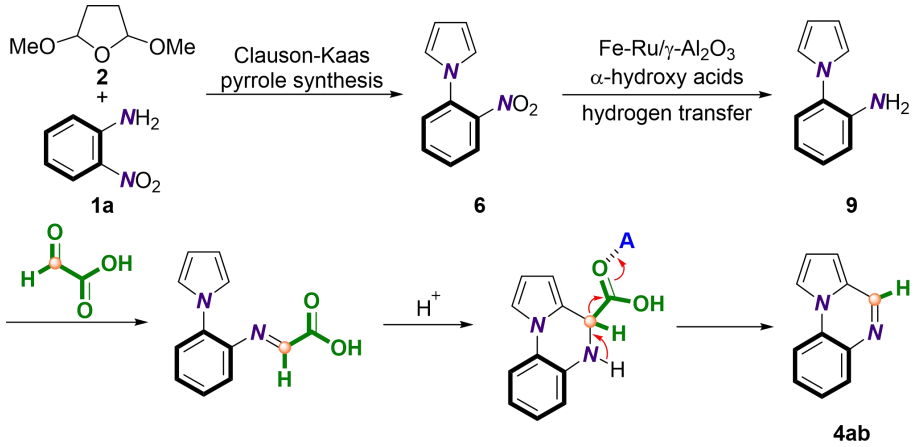

Scheme S5. Plausible reaction pathway for the further conversion of mixed acids

3.4 Synthesis of Fluorescent Molecular and Its Applications

One pot two steps procedure (Scheme 8): The pressure tube was filled with 2-nitro aniline (**1a**, 0.10 mmol), 2,5-dimethoxytetrahydrofuran (**2a**, 0.15 mmol), lactic acid (**3a**, 0.3 mL), the reaction mixture was stirred at 140 °C under air for 12 h. Afterwards, 4-(dimethyl-lamino)benzaldehyde (**7**, 14.9 mg, 0.10 mmol), Et_3N (4.0 equiv.), anhydrous acetic anhydride (1.0 mL) and Fe-Ru/γ-Al_2O_3 (5.0 mg) were added. The reaction mixture was stirred at 140 °C under microwave for 2 min. After cooling to room temperature, the mixture was removed under reduced pressure. The residue was purified by flash silica gel chromatography to afford the desired product **8** as a reddish-brown solid (10.1 mg, 32% yield).

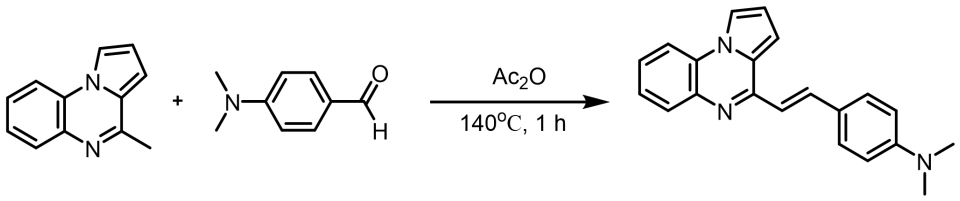

Scheme S6. Post -synthesis of fluorescent molecular **8**

A pressure tube was charged with acetic anhydride (1 mL), **4aa** (18.2 mg, 0.10 mmol) and 4-(dimethyl-lamino)benzaldehyde (**7**, 14.9 mg, 0.10 mmol). The reaction mixture was stirred at 140 °C for 1 h under air condition. After cooling to room temperature, the mixture was quenched through saturated sodium bicarbonate solution, and then were extracted with ethyl acetate. The residue was purified by silica gel chromatography to afford the product **8** as a reddish-brown solid (23.8 mg, 76% yield) (Scheme S6).

^{1}H NMR (400 MHz, chloroform-*d*): δ = 8.10 (d, *J* = 15.8 Hz, 1H), 8.02 (dd, *J* = 6.1, 3.4 Hz, 1H), 7.92 (d, *J* = 2.9 Hz, 1H), 7.80 (dd, *J* = 6.2, 3.4 Hz, 1H), 7.61 (d, *J* = 8.3 Hz, 2H), 7.42 (dd, *J* = 6.3, 3.4 Hz, 2H), 7.31 (d, *J* = 15.8 Hz, 1H), 7.12 (d, *J* = 4.1 Hz, 1H), 6.89 (t, *J* = 3.5 Hz, 1H), 6.73 (d, *J* = 8.4 Hz, 2H), 3.02 (s, 6H) ppm. ^{13}C NMR (101 MHz, chloroform-*d*): δ = 151.2, 150.4, 137.7, 136.0, 129.4, 129.2, 127.1, 126.5, 126.1, 125.4, 124.4, 117.7, 114.6, 113.8, 113.7, 112.1, 106.3, 40.3 ppm.

Applications: The fluorescence were measured in different solvents, Interestingly, the compound emits in the green region and shows bright fluorescence in viscous glycerol. The fluorescence emission was further studied with varying water fractions (f_w) in the MeCN/water mixture, making it the promising material as a novel TICT-based fluorophore. Moreover, their abilities to penetrate cell membranes, and selectively accumulate in the cytoplasm was demonstrated, indicating their potential applications in cell imaging.

The product **8** was dissolved in DMSO to prepare a 10 mmol/L masterbatch, which was then diluted with 12 different solvents to a concentration of 10 μmol/L and tested for fluorescence intensity, respectively (Figure 6a).

The compound **8** was dissolved in acetonitrile to prepare a 10 mmol/L master solution, which was then diluted into mixed solutions of acetonitrile and water with different water contents at a concentration of 20 μmol/L, and the fluorescence intensity was tested (Figure 6b).

Cell culture and fluorescence imaging HeLa cells were used for fluorescence imaging. The cells were cultured in Dulbecco's Modified Eagle Medium (DMEM) supplemented with 10% fetal bovine serum (FBS) at 37 ^{o}C with 5% CO_2 incubation. The cells used for fluorescence imaging were stained with the compound (10 μM) for 1 h and washed with PBS. The cell images were obtained by using a Carl Zeiss LSM800 CLSM with a 63 × objective. λ_{ex} = 488 nm, λ_{em} = 500–600 nm (Figure 6c).

IV. Mechanism studies

4.1 Product distribution as a function of time

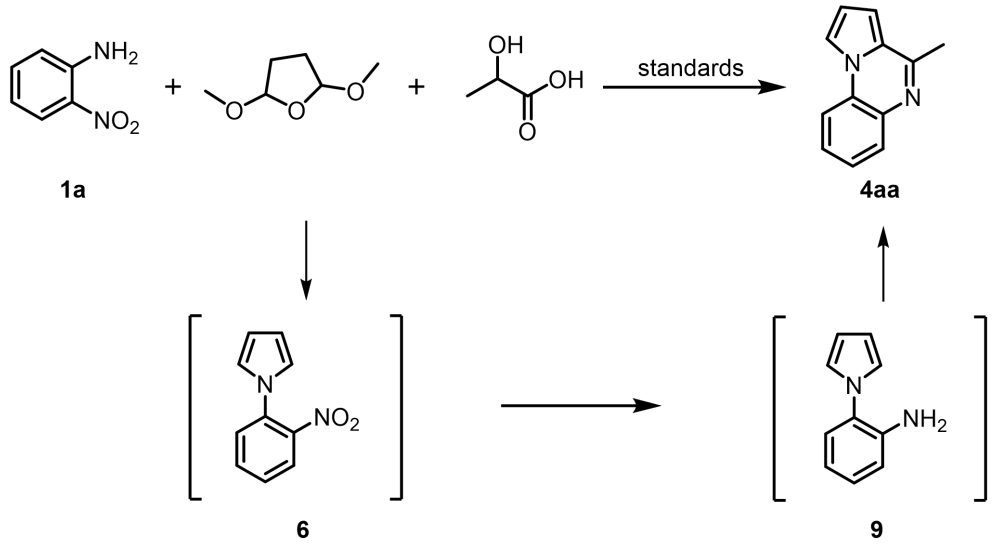

A pressure tube was charged with Fe-Ru/*γ*-Al_2O_3 (5.0 mg), 2-nitroaniline **1a** (13.8 mg, 0.10 mmol), 2,5-dimethoxytetrahydrofuran (**2**, 13.9 mg, 0.15 mmol), triethylamine (40.4 mg, 0.4 mmol), and lactic acid (**3a**, 0.3 mL). The reaction mixture was stirred at 140 °C for the indicated time (ten parallel runs). The reactions were monitored by ^{1}H NMR at 1 min, 5 min, 10 min, 20 min, 30 min, 60 min, 90 min, 180 min, 270 min, and 360 min to obtain the proportion of the crude product using 1,3,5-trimethoxybenzene as an internal standard (Table S5, Figure S4).

Table S5. Kinetic studies on the conversion of **1a** to **4aa**

Time (min)	Remaining of **1a** (%)	Yield of **9** (%)	Yield of **6** (%)	Yield of **4aa** (%)
1	45	0	55	0
5	6	0	94	0
10	2	0	94	0
20	0	0	93	0
30		10	84	6
60		11	60	25
90		13	50	39
180		13	28	55
270		10	18	66
360		6	8	75

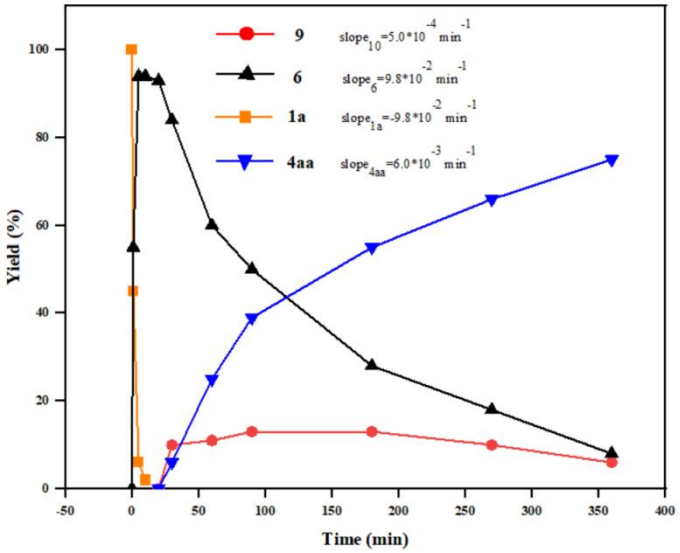

Figure S4. The plots of yield against time for the reaction process from **1a** to **4aa**

4.2 Control Experiments

(a) ***Radical trapping experiments***

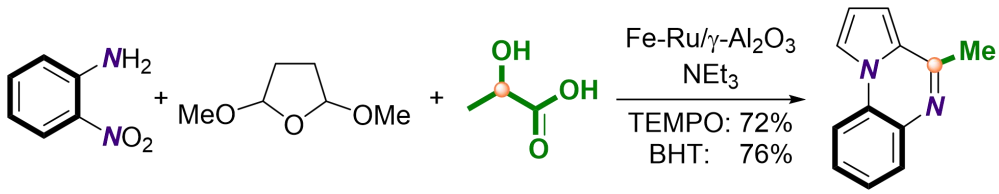

1a **2** **3a** **4aa**

The radical trapping experiment was carried out as follows: 1.0 equiv. of TEMPO (2,2,6,6-tetramethylpiperidin 1-oxyl) or BHT (2,6-di-*tert*-butyl-4-methylphenol) was subjected to the reaction mixture of 2-nitroaniline (**1a**), 2,5-dimethoxyltetrahydrofuran (**2**), and lactic acid (**3a**) under standard reaction conditions, the reaction was not inhibited in either case.

(b) ***The effect of different acid in Clauson-Kaas reaction***

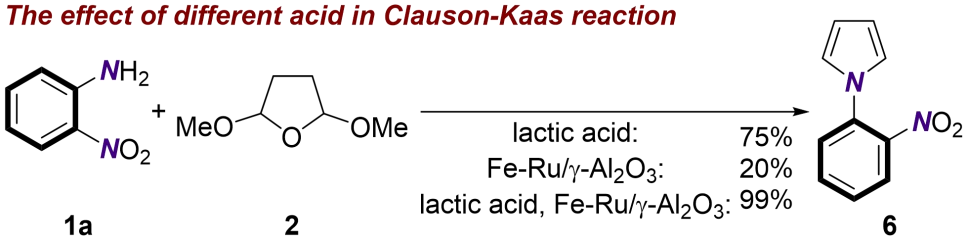

1a **2** **6**

To a pressure tube, 2-nitroaniline (**1a**, 0.10 mmol) and 2,5-dimethoxyltetrahydrofuran (**2**, 0.12 mmol) were employed in lactic acid (**3a**, 0.3 mL) to give 2-nitrophenyl pyrrole (**6**) in 75% yield. In addition, **1a** and **3a** conducted in H_2O under Fe-Ru/γ-Al_2O_3 (5.0

mg) catalysis afforded product **6** in 20% yield. By comparison, **6** was obtained in 99% yield in the presence of 5.0 mg Fe-Ru/*γ*-Al_2O_3 and 0.3 mL lactic acid.

The investigation of the hydrogen source

(c)

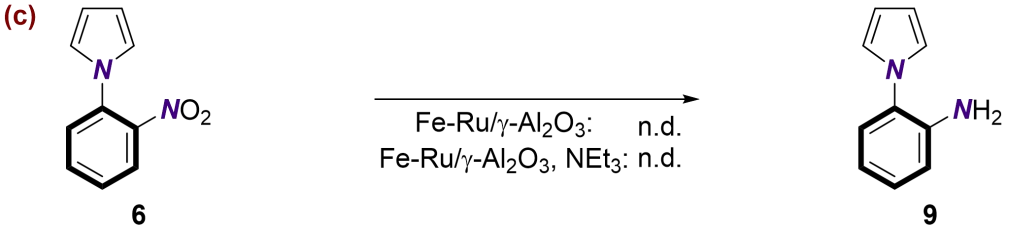

6 **9**

2-Nitrophenyl pyrrole (**6**, 0.10 mmol) was subjected to the reaction under Fe-Ru/*γ*-Al_2O_3 in absence of lactic acid, no desired product **9** was observed in this case or even in the presence of triethylamine (Et_3N).

(d)

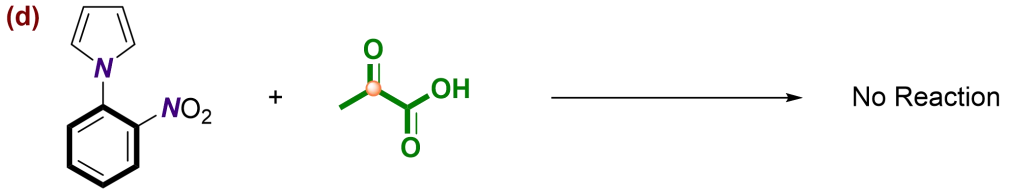

6 **10**

A pressure tube was charged with 2-nitrophenyl pyrrole (**6**, 0.10 mmol), pyruvic acid (**10**, 0.3 mL), Et_3N (0.4 mmol), and Fe-Ru/*γ*-Al_2O_3 (5.0 mg), the mixture was stirred at 140 °C for 6 h, however, no conversion was observed.

The influence of cascade reaction

(e)

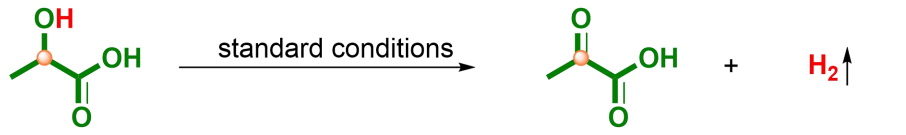

3a **10** 0.042 mmol

A pressure tube was charged with lactic acid (**3a**, 0.3 mL) and Fe-Ru/*γ*-Al_2O_3 (5.0 mg), the mixture was stirred at 140 °C for 6 h, 0.042 mmol H_2 was observed accompanied by the generation of **10**.

Hydrogen with a volume of 0.1 mL, 0.3 mL, 0.5 mL, 0.7 mL, and 0.9 mL was injected into the reaction vessel containing the template reaction system, and the volume of 1.0 mL above the liquid surface of the system was extracted and injected into the gas chromatography for analysis, and the peak area corresponding to each hydrogen concentration was recorded (Table S6). A standard curve is plotted based on the

hydrogen concentration in the sample tube and the corresponding peak area (Figure S5). The established standard curve was used to analyze the sample to be tested, and the concentration of the target compound in the sample was calculated by back-extrapolating the standard curve according to the peak area of the sample.

Table S6. Peak area for different volumes of hydrogen

H_2 (mL)	Area (uV*s)
0.1	1320.74
0.3	74061.81
0.5	129444.36
0.7	186826.91
0.9	238209.46

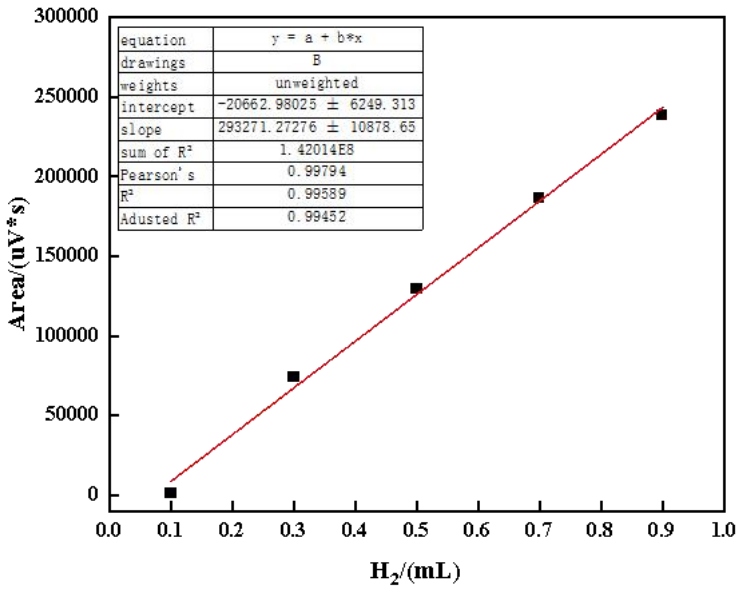

Figure S5. Standard curve equation

According to standard curve equations (Figure S5), 0.042 mmol H_2 release was observed by GC (Table S7, Figure S6).

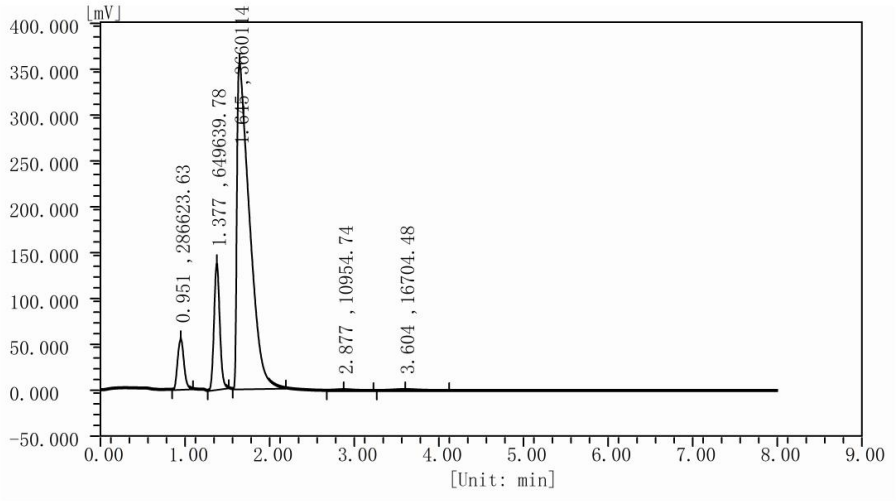

Figure S6. GC analysis on hydrogen products

Table S7. GC analysis results

Molecule	Time (min)	High (uV)	Area (uV*s)
H_2	0.951	55056.3	286623.6

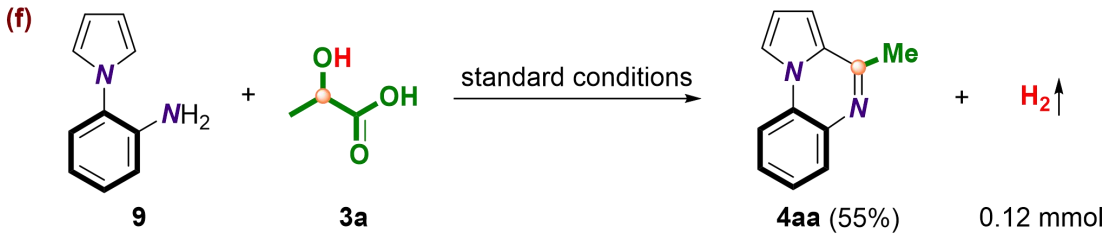

9 **3a** **4aa** (55%) 0.12 mmol

According to the **GP**, 2-(1*H*-pyrrol-1-yl)aniline (**9**, 0.10 mmol) and lactic acid (**3a**, 0.3 mL) were employed under standard reaction conditions, **4aa** was obtained in 55% yield accompanied by 0.11 mmol of H_2.

Based on the standard curve equation (Figure S5), **4aa** was obtained in 55% yield accompanied by 0.11 mmol of H_2 (Table S8, Figure S7).

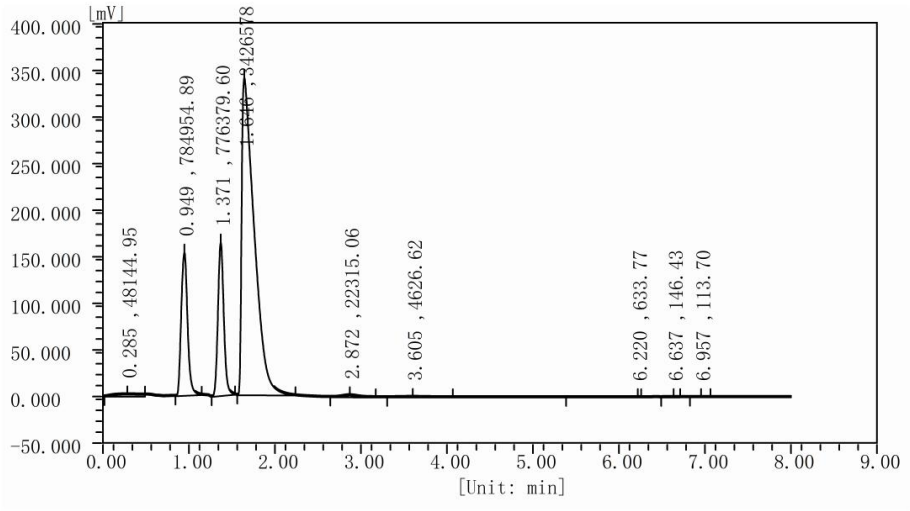

Figure S7. GC analysis on hydrogen products

Table S8. GC analysis results

Molecule	Time (min)	High (uV)	Area (uV*s)
H_2	0.949	153554.4	784954.9

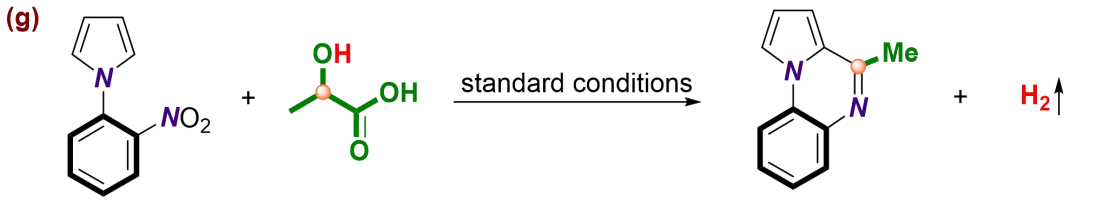

6 **3a** **4aa** (90%) 0.21 mmol

2-Nitrophenyl pyrrole (**6**, 0.10 mmol) and lactic acid (**3a**, 0.3 mL) were employed under standard reaction conditions, desired product **4aa** was obtained in 90% yield accompanied by 0.21 mmol of H_2.

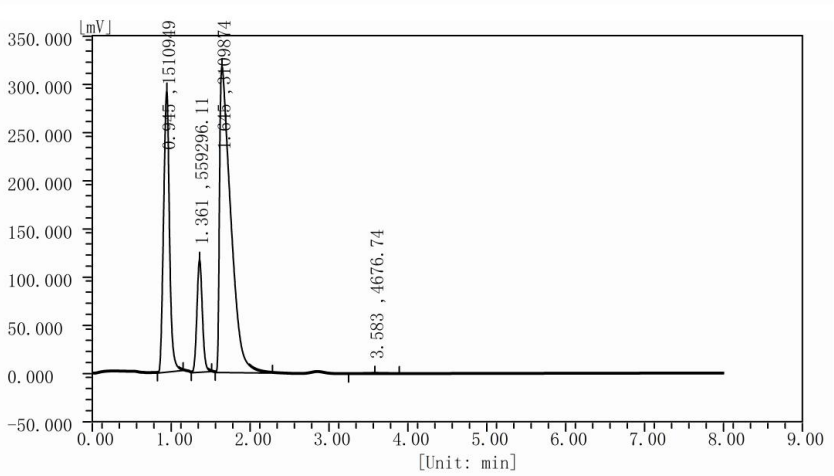

Figure S8. GC analysis on hydrogen products

Based on standard curve equations (Figure S5), **4aa** was obtained in 90% yield accompanied by 0.21 mmol of H_2 (Table S9, Figure S8).

Table S9. GC analysis results

Molecule	Time (min)	High (uV)	Area (uV*s)
H_2	0.945	291901.0	1510949.0

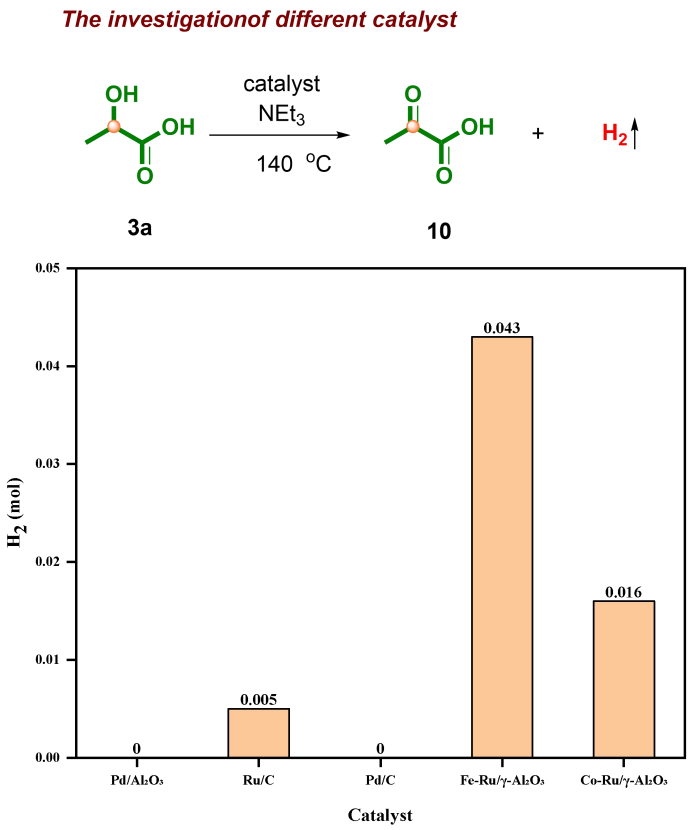

Figure S9.. Hydrogen content released with different catalysts

The pressure tube was filled with lactic acid (**3a**, 0.3 mL), Et_3N (4.0 equiv.) and heterogeneous catalyst: Pd/Al_2O_3, Ru/C, Pd/C, and Co-Ru/γ-Al_2O_3 (20 mg). The reaction mixture was stirred at 140 °C for indicated time. The H_2 release was observed by gas chromatography and calculated according to the standard curve equation (Table S10, Figures S9–S13).

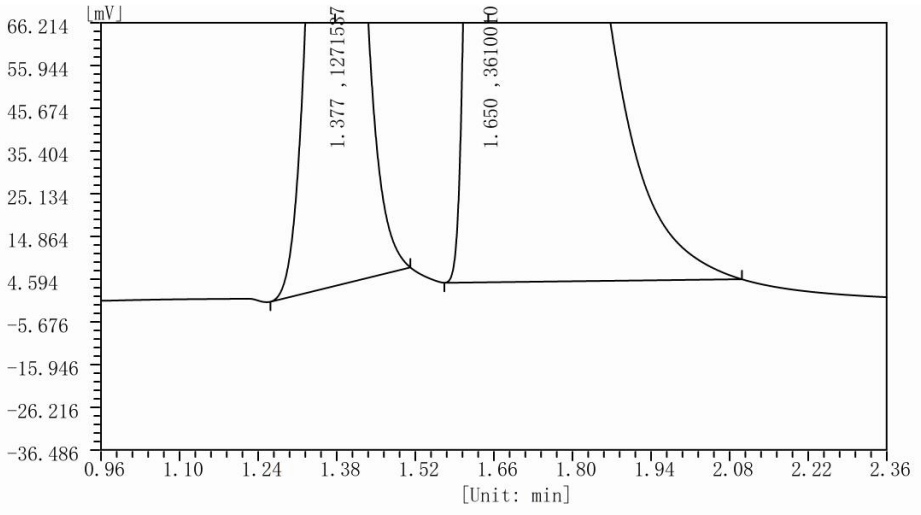

Figure S10. GC analysis on hydrogen products with Pd/Al_2O_3

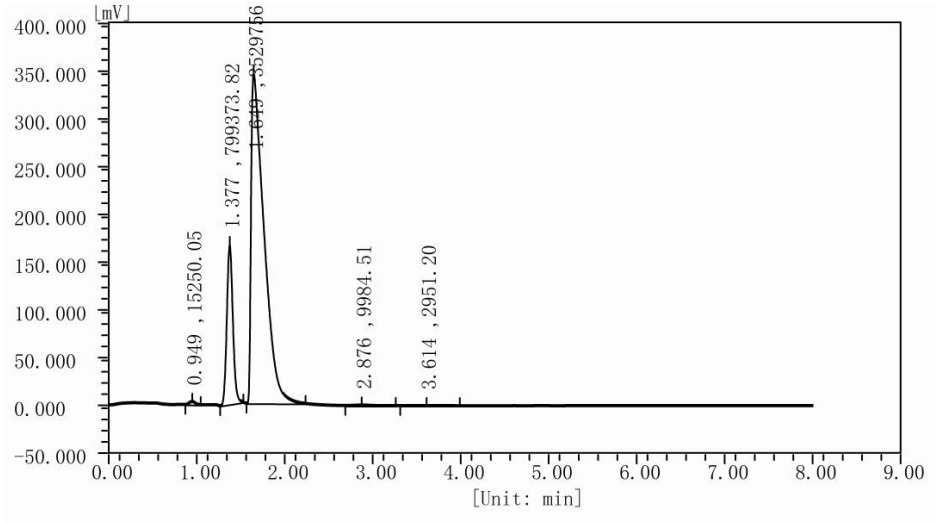

Figure S11. GC analysis on hydrogen products with Ru/C

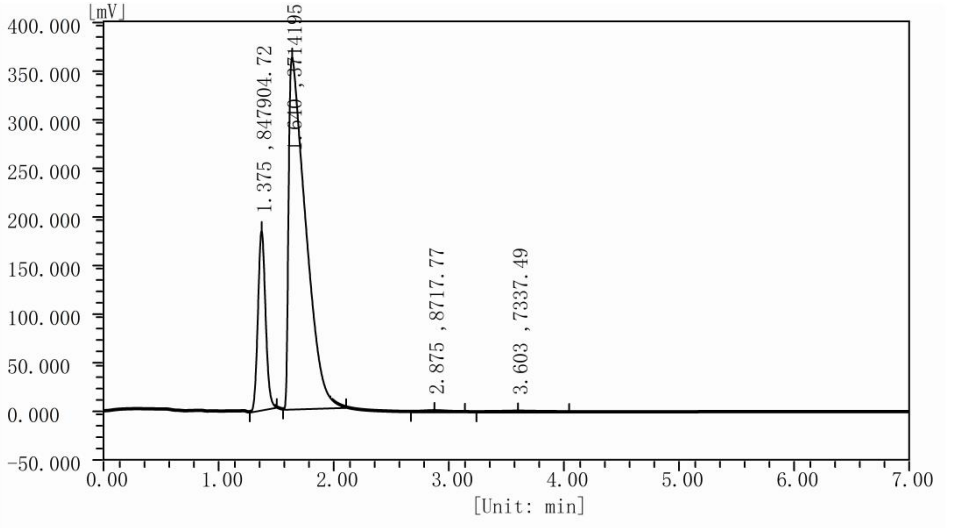

Figure S12. GC analysis on hydrogen products with Pd/C

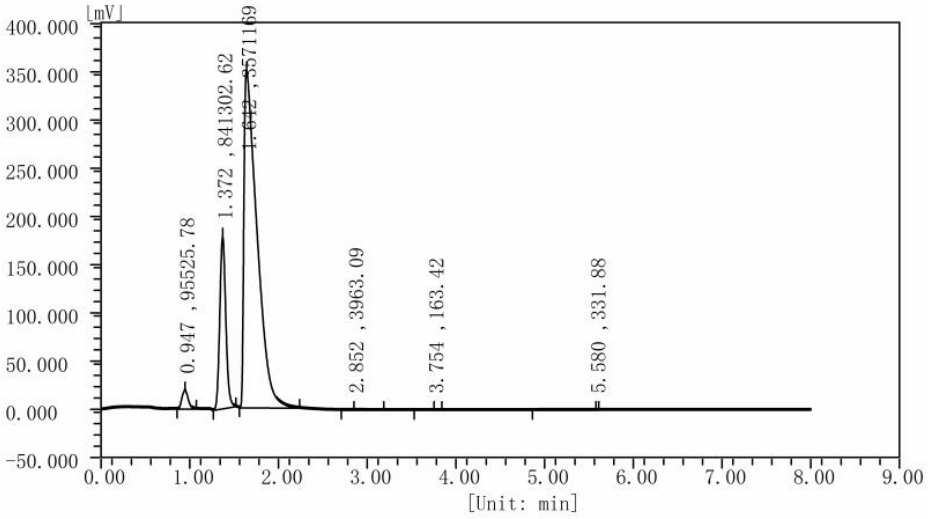

Figure S13. GC analysis on hydrogen products with Co-Ru/*γ*-Al_2O_3

Table S10. GC analysis results with different catalysts

Catalysts	Molecule	Time (min)	High (uV)	Area (uV*s)
Pd/Al_2O_3	H_2	/	0	0
Ru/C		0.949	3236.2	15250.05
Pd/C		/	0	0
Co-Ru/*γ*-Al_2O_3		0.947	19053.9	95525.78

(h) ***The effect of catalyst in the cyclization***

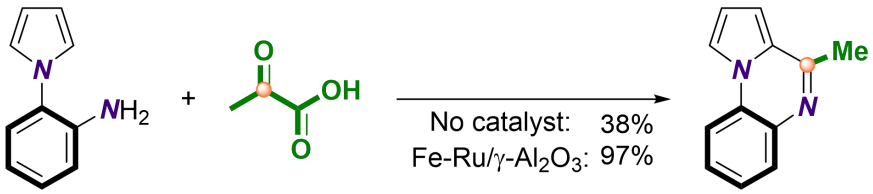

9 **10** **4aa**

A pressure tube was charged with 2-(1*H*-pyrrol-1-yl)aniline (**9**, 0.10 mmol) and pyruvic acid (**10**, 0.3 mL), after stirring at 140 °C for 6 h, the cyclized product was provided in 38% yield. By comparison, the desired product **4aa** was achieved up to 97% yield in the presence of Fe-Ru/*γ*-Al_2O_3 (5.0 mg).

4.3 Reaction System Determination

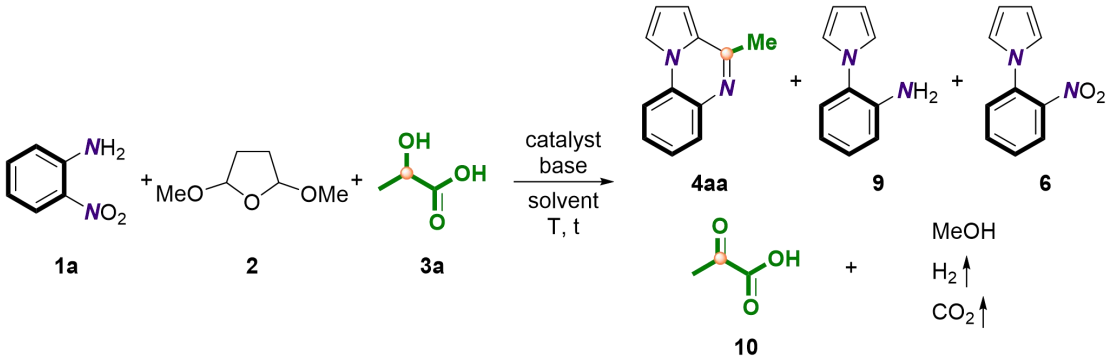

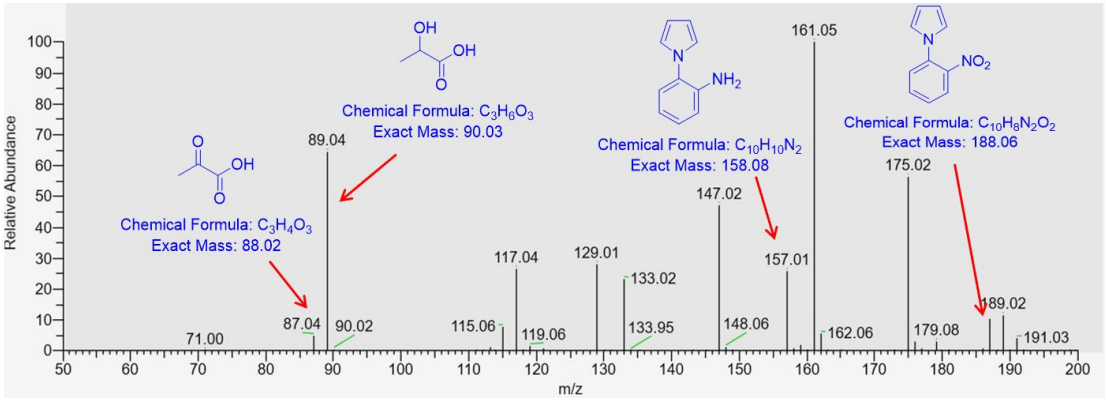

Figure S14. ESI-MS spectra (negative ion mode) of the crude catalytic system

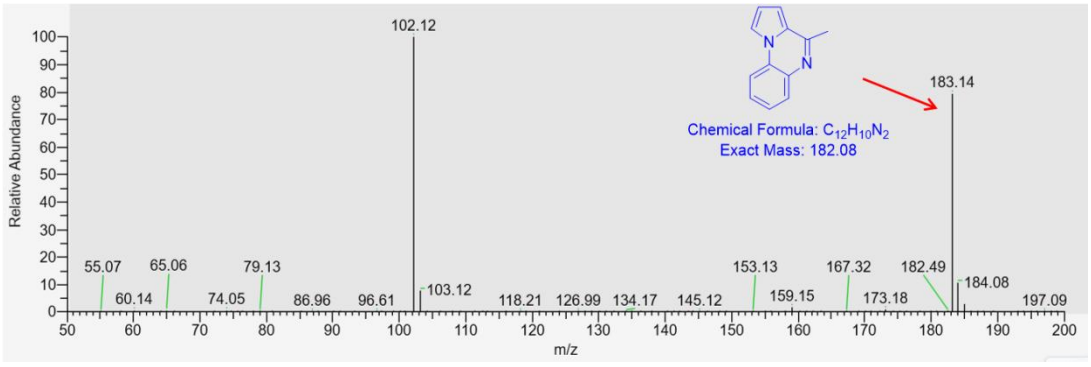

Figure S15. ESI-MS spectra (positive ion mode) of the crude catalytic system

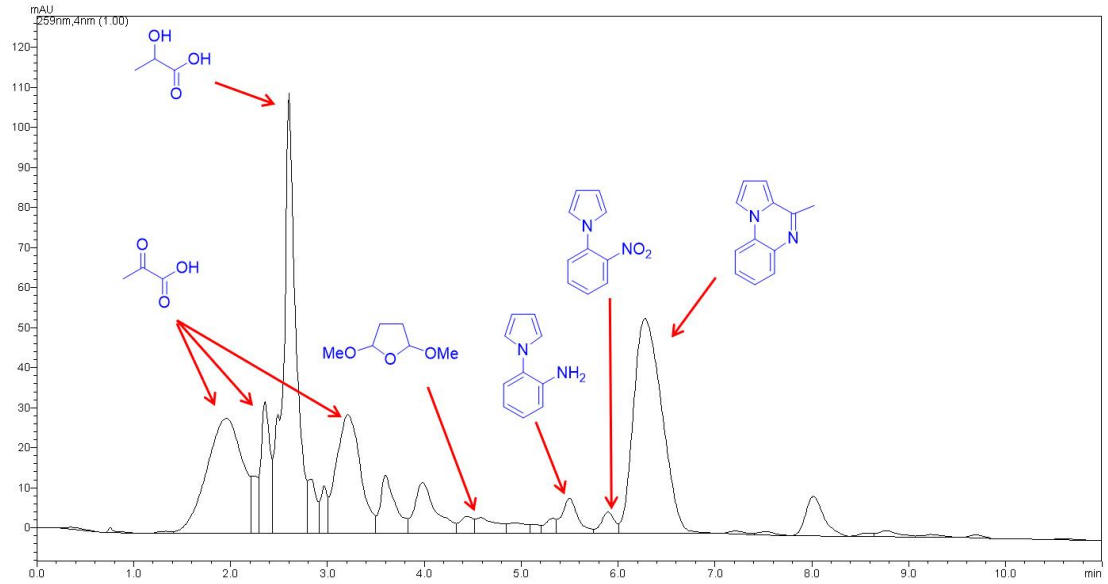

Figure S16. HPLC spectra of the crude catalytic system

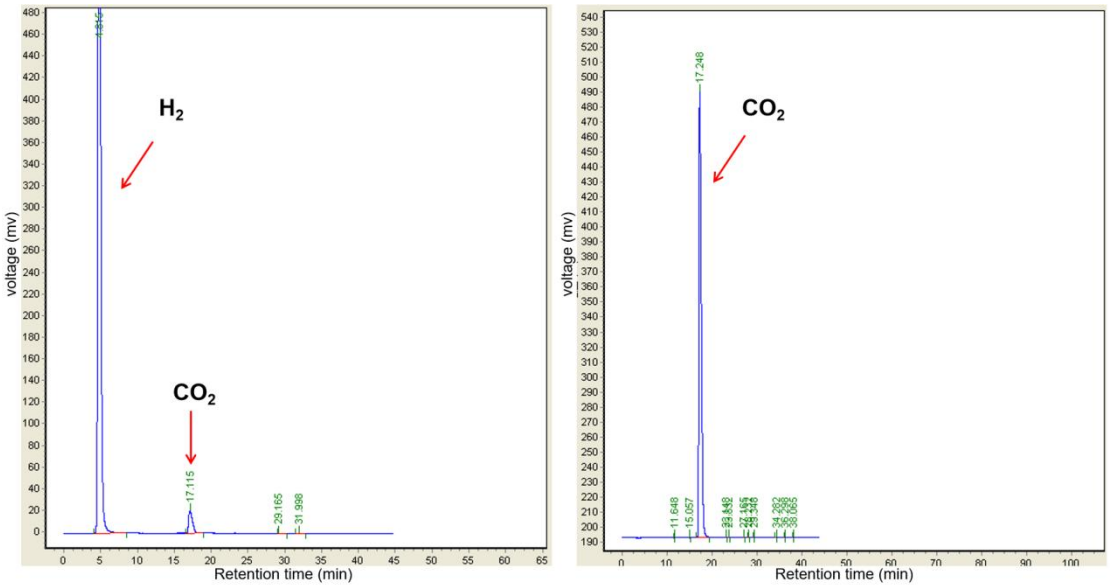

Figure S17. GC spectra of the gas phase in the catalytic system

4.4 Acidity Determination of the Catalyst

The acidic properties of the Fe-Ru/γ-Al_2O_3 catalyst was detected by temperature programmed desorption of ammonia (NH_3-TPD), and the corresponding profile is displayed in Figure S18. Obviously, the spectra exhibited several NH_3 desorption peaks, in which the peaks of the lower temperature centred in the range of 90–245 °C are attributed to physisorbed NH_3 on weak acid sites. On the other hand, the desorption peaks of high temperature at 245–360 °C are related to medium and strong acid sites due to the hydrogen-bonded NH_3. The acidic sites for 50–200 °C and

200–500 °C are determined to be 0.087 and 0.158 mmol/g, respectively (Table S11).

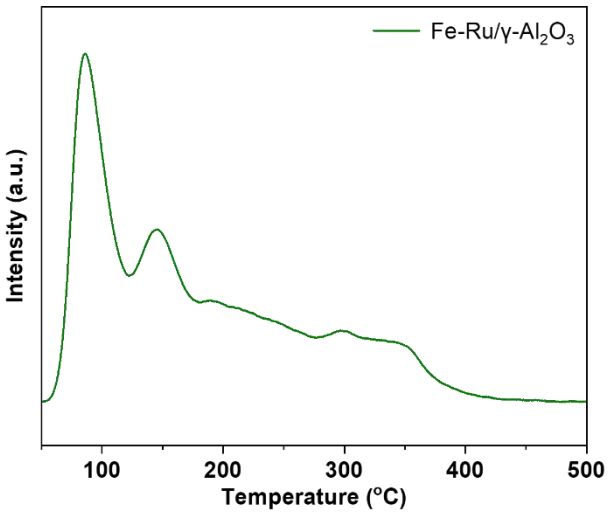

Figure S18. NH_3-TPD profile of Fe-Ru/*γ*-Al_2O_3.

Table S11. NH_3-TPD data

Entry	Start temp. (°C)	End temp. (°C)	Temp. width (°C)	Area (count)	mmol	mmol/g
1	50.0	200.0	150	258.01	0.016	0.158
2	200.0	500.0	300	142.59	0.009	0.087

V. ^{1}H and ^{13}C NMR Spectra of the Products

^{1}H NMR spectrum of compound **4aa** (400 MHz, $CDCl_3$)

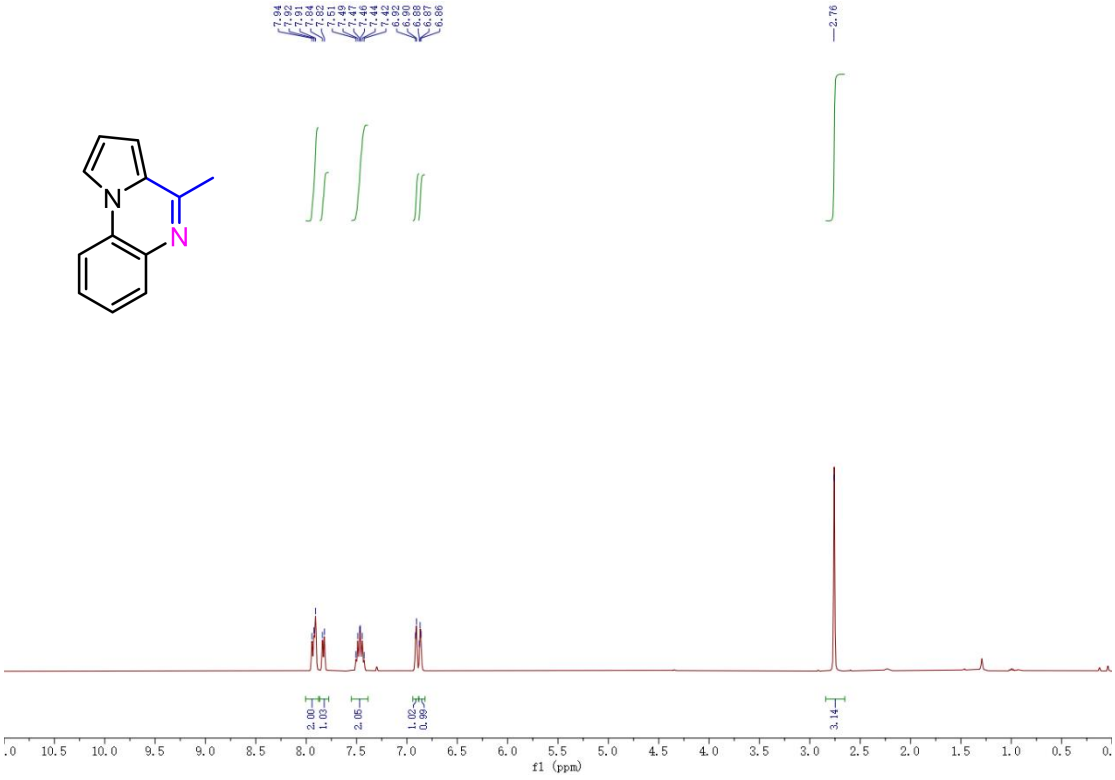

^{13}C NMR spectrum of compound **4aa** (101 MHz, $CDCl_3$)

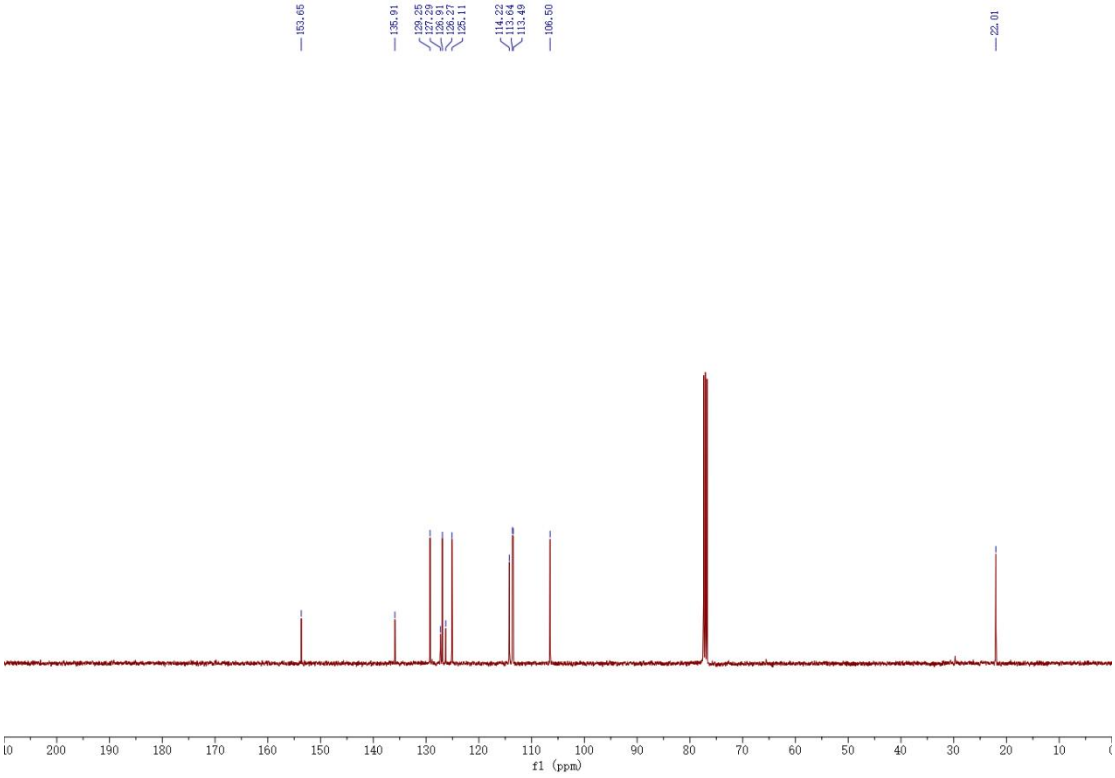

^{1}H NMR spectrum of compound **4ba** (400 MHz, $CDCl_3$)

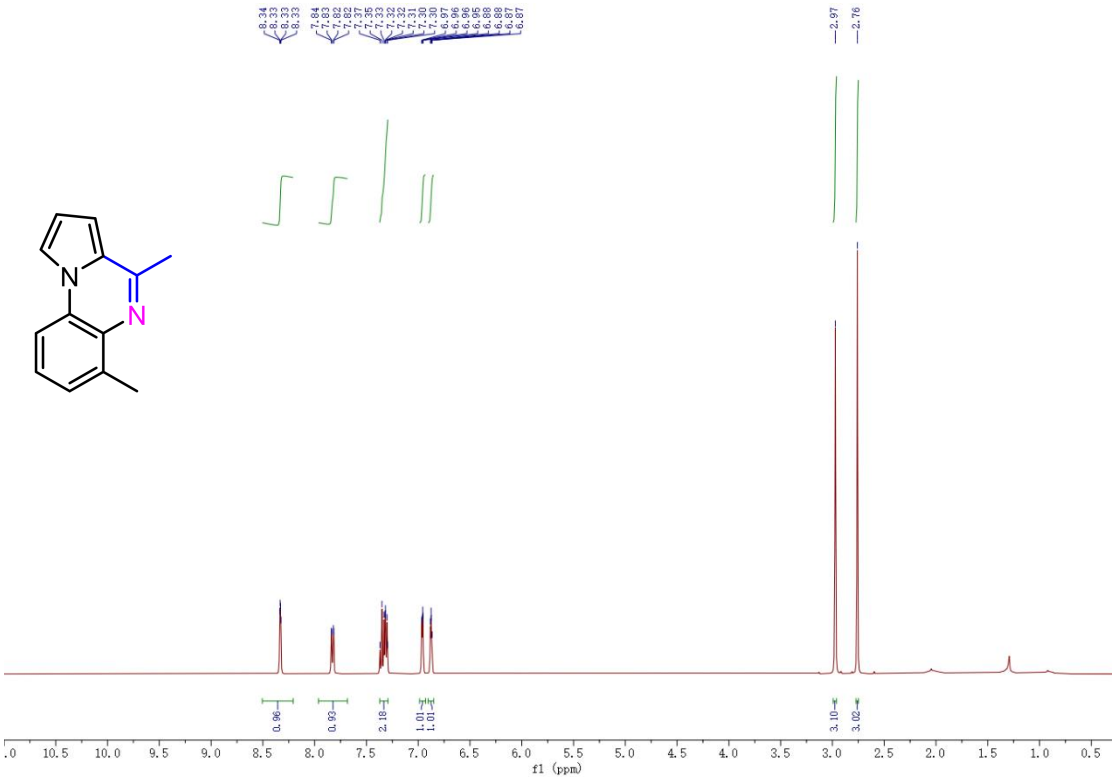

^{13}C NMR spectrum of compound **4ba** (101 MHz, $CDCl_3$)

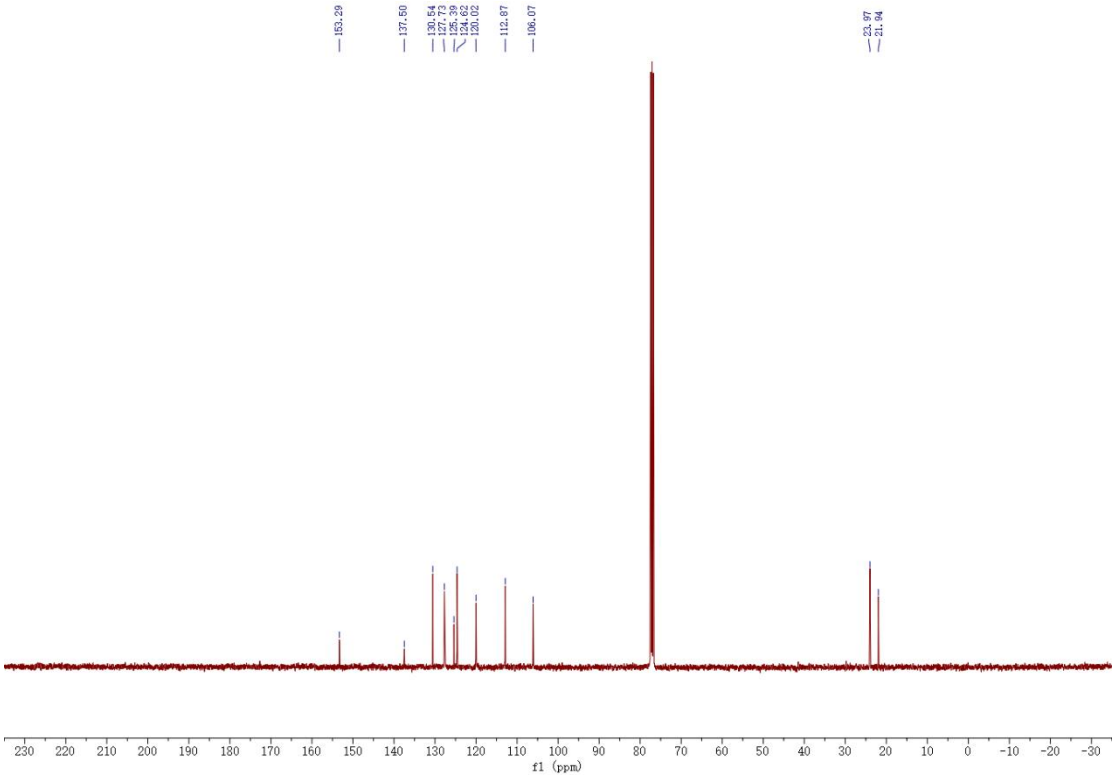

^{1}H NMR spectrum of compound **4ca** (400 MHz, $CDCl_3$)

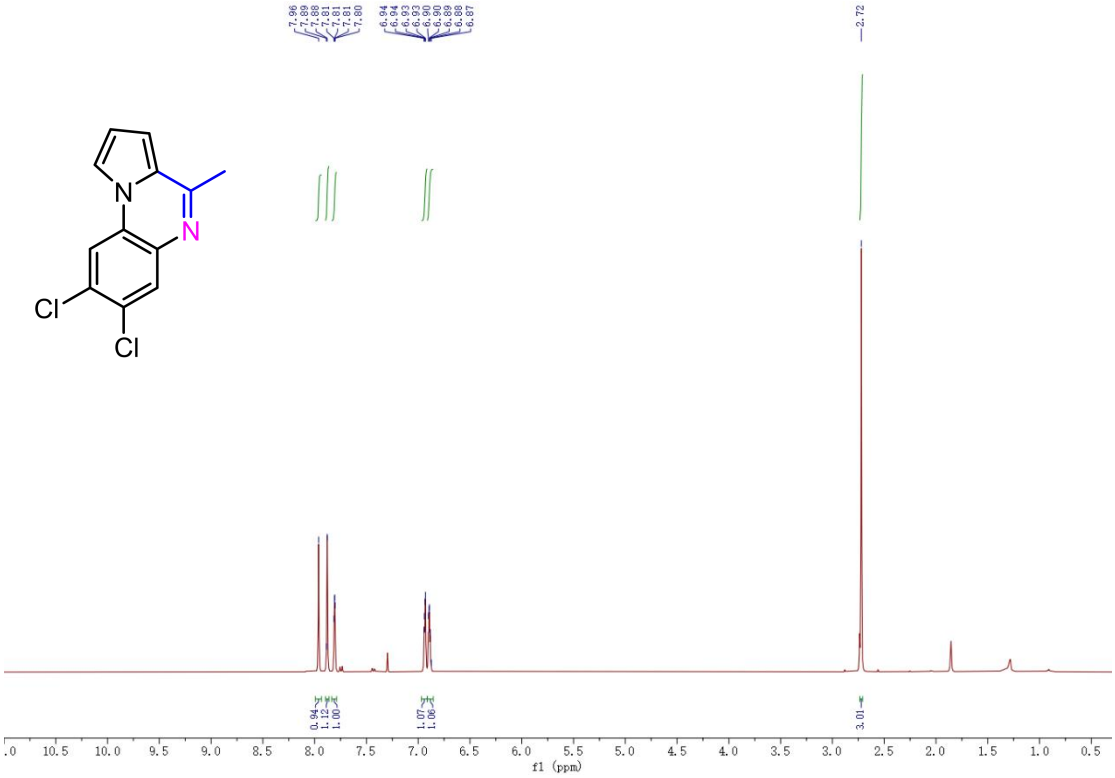

^{13}C NMR spectrum of compound **4ca** (101 MHz, $CDCl_3$)

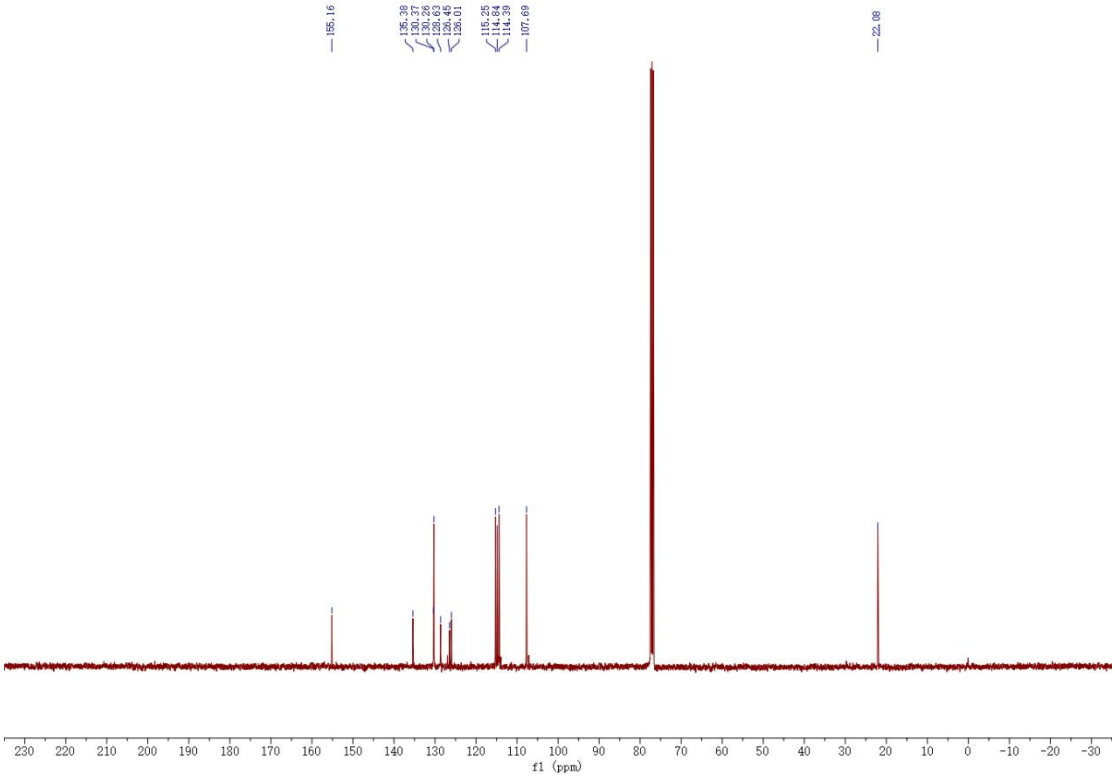

^{1}H NMR spectrum of compound **4da** (400 MHz, $CDCl_3$)

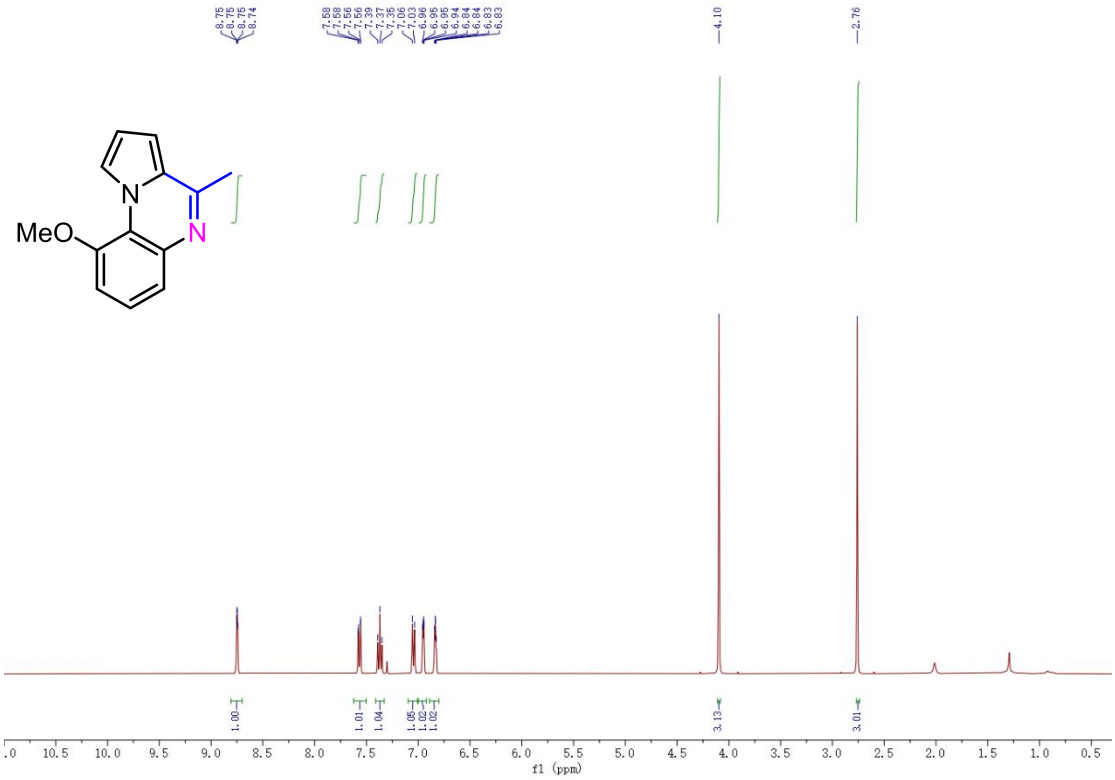

^{13}C NMR spectrum of compound **4da** (101 MHz, $CDCl_3$)

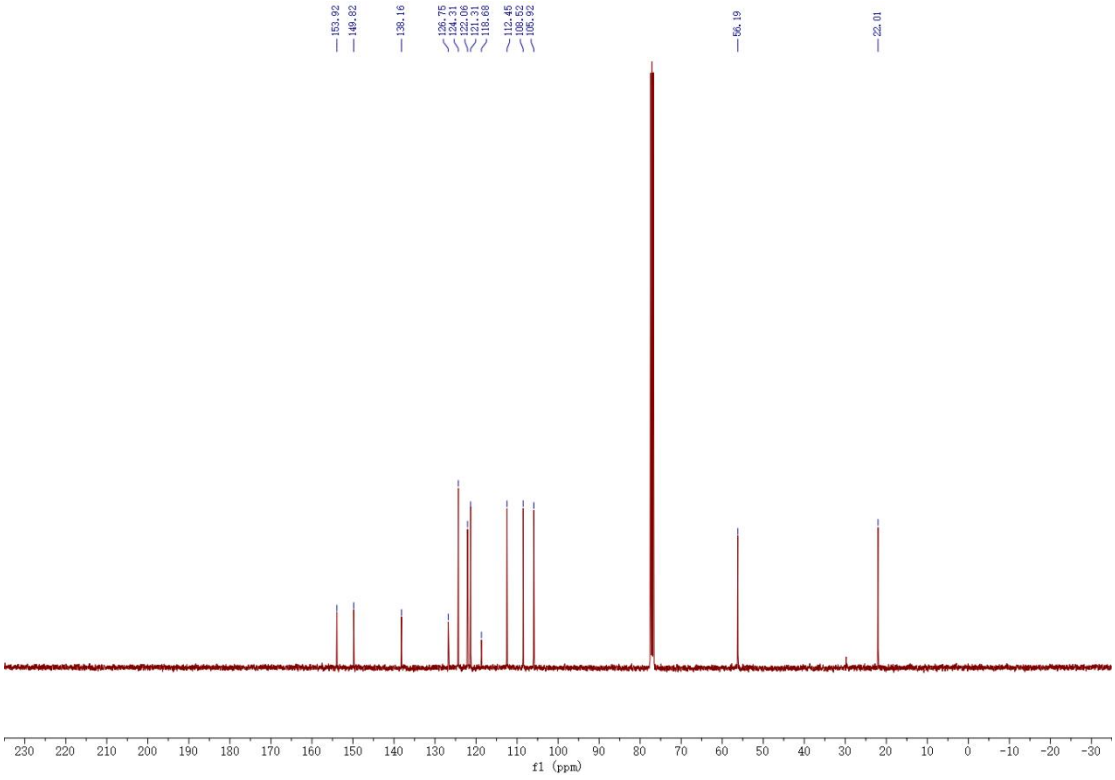

^{1}H NMR spectrum of compound **4ea** (400 MHz, $CDCl_3$)

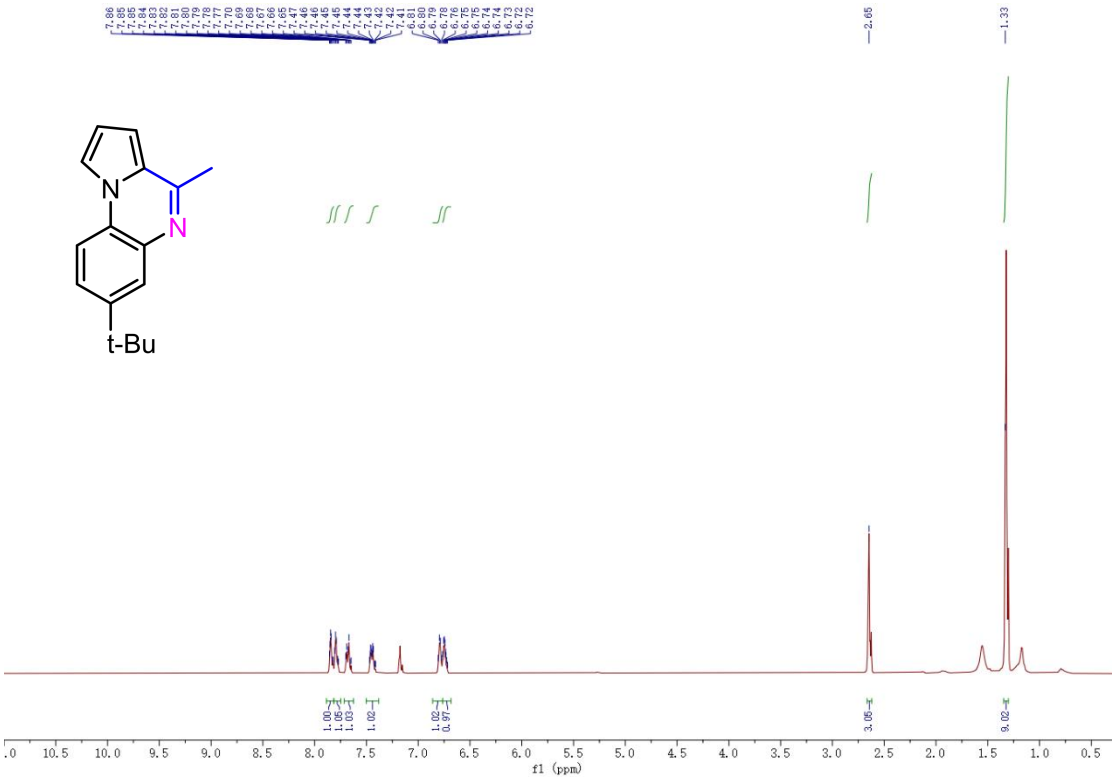

^{13}C NMR spectrum of compound **4ea** (101 MHz, $CDCl_3$)

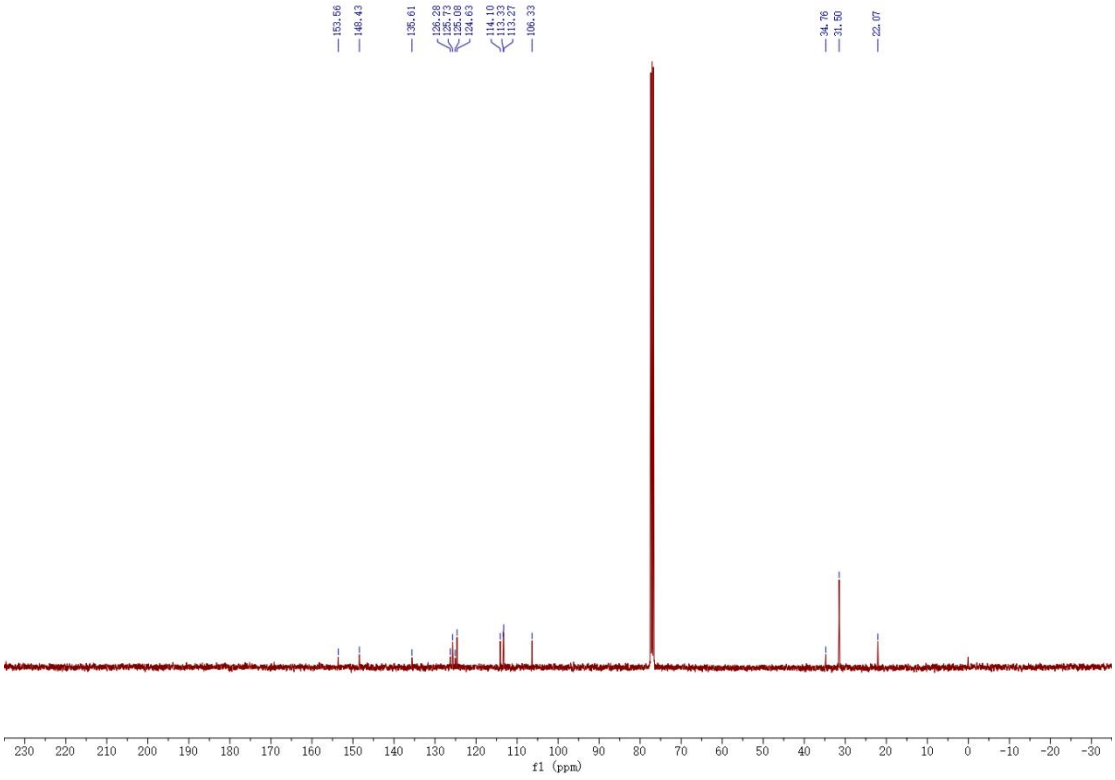

^{1}H NMR spectrum of compound **4fa** (400 MHz, $CDCl_3$)

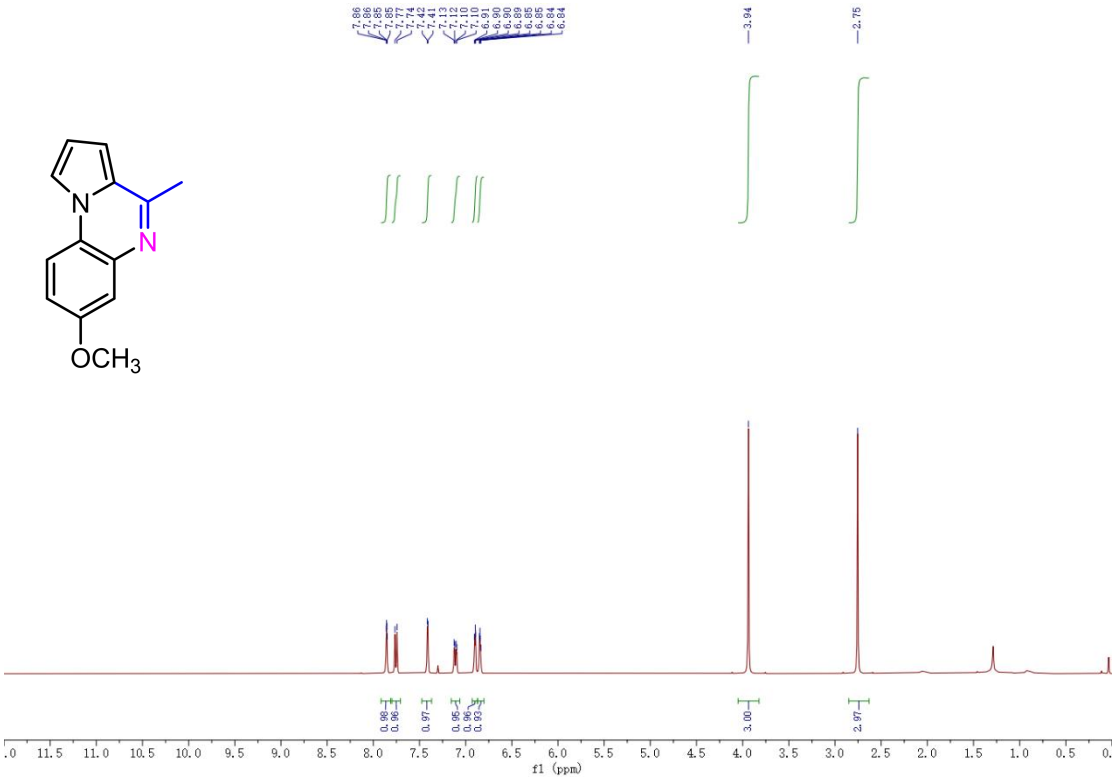

^{13}C NMR spectrum of compound **4fa** (101 MHz, $CDCl_3$)

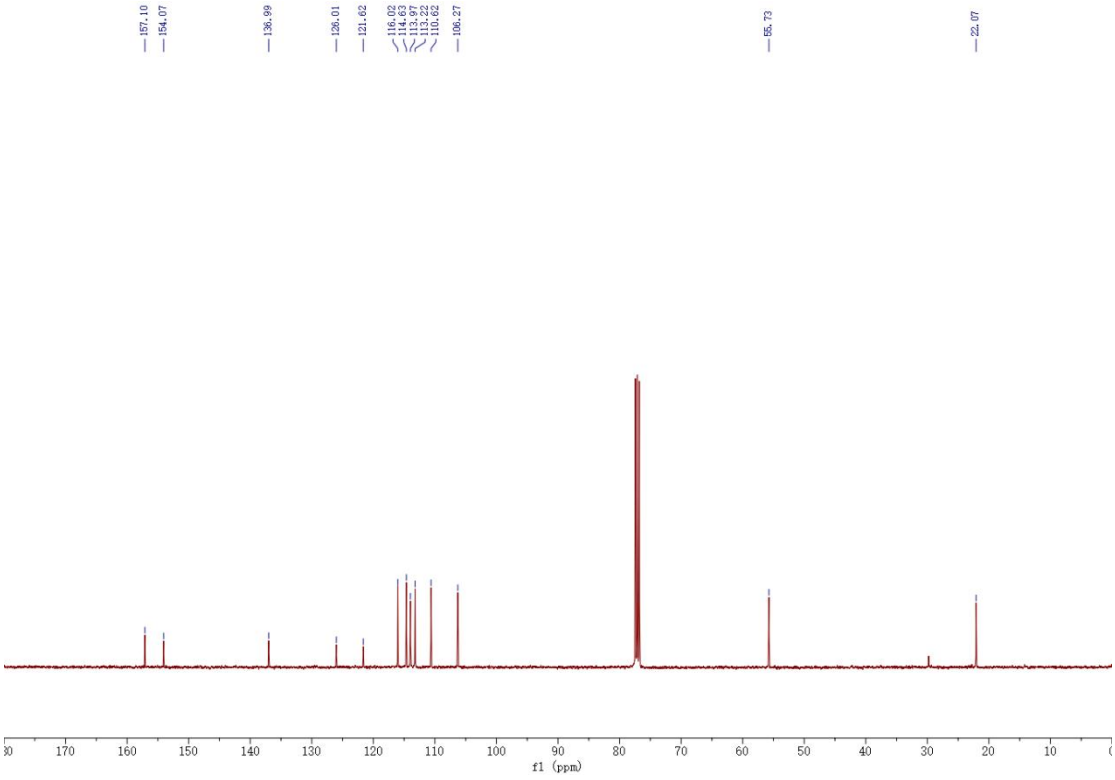

^{1}H NMR spectrum of compound **4ga** (400 MHz, $CDCl_3$)

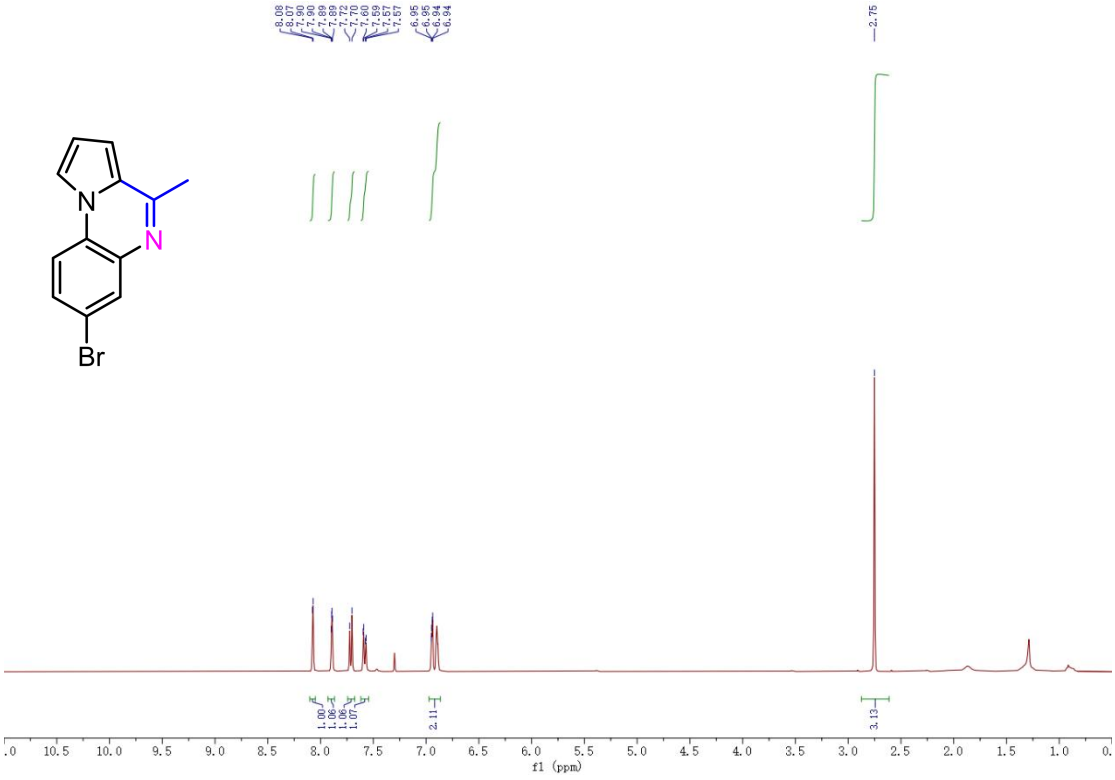

^{13}C NMR spectrum of compound **4ga** (101 MHz, $CDCl_3$)

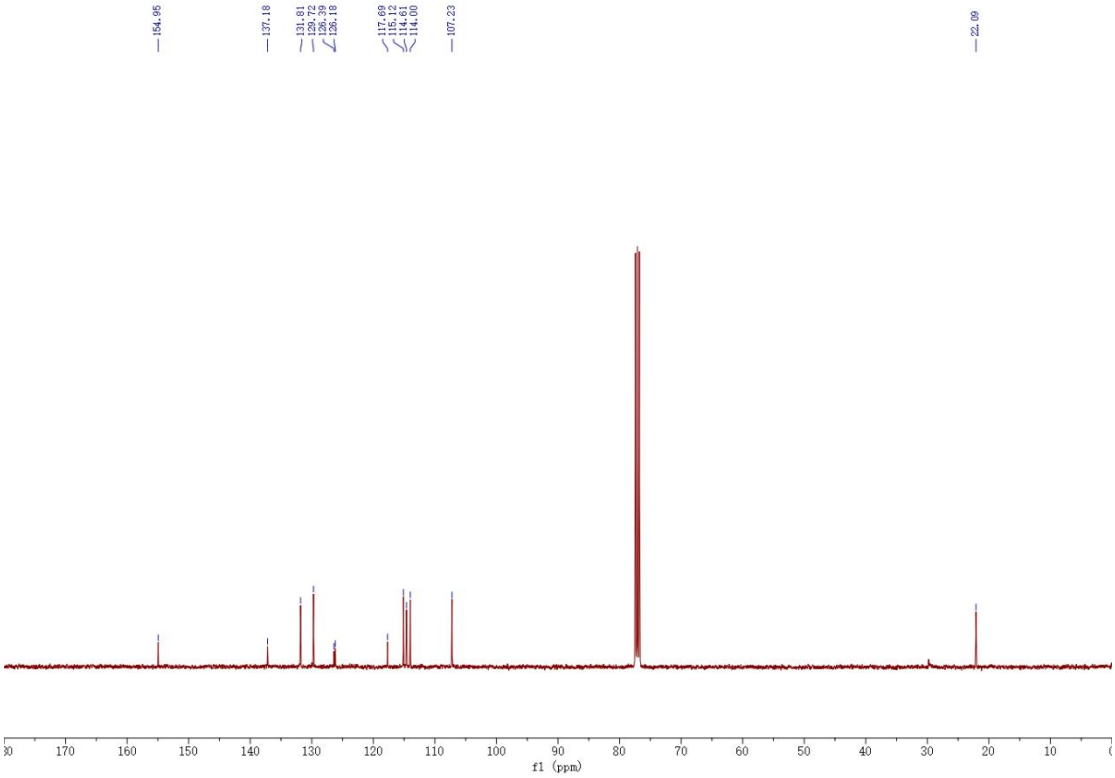

^{1}H NMR spectrum of compound **4ha** (400 MHz, $CDCl_3$)

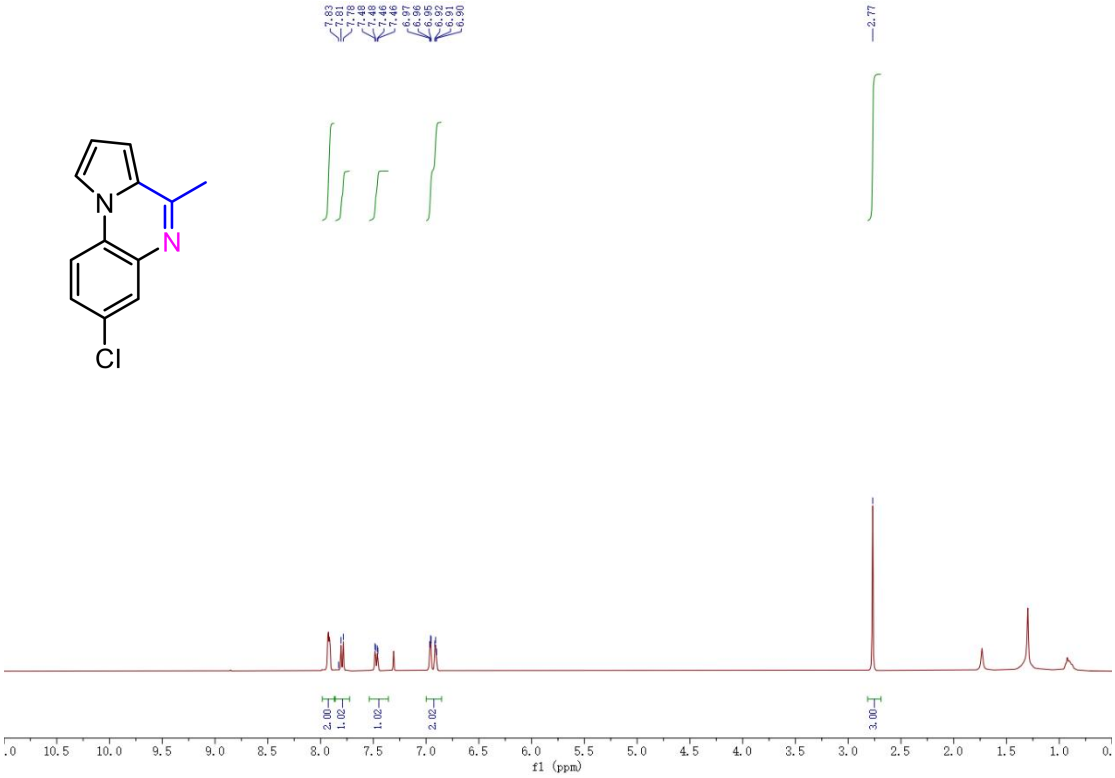

^{13}C NMR spectrum of compound **4ha** (101 MHz, $CDCl_3$)

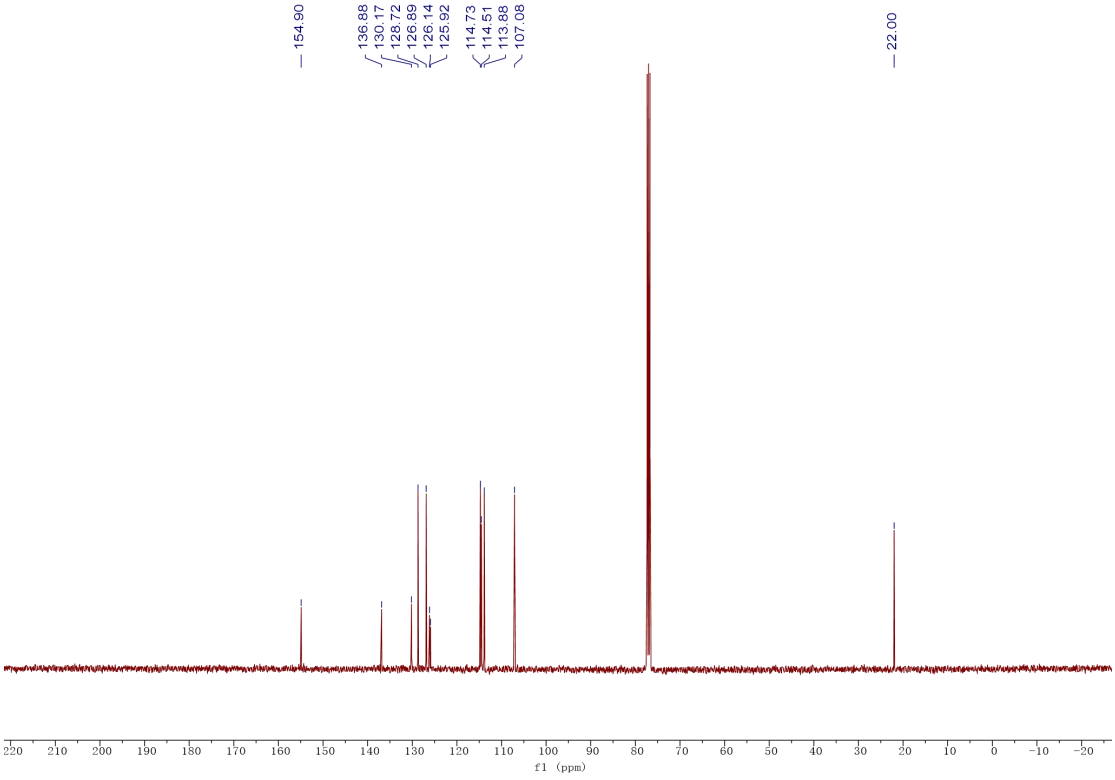

^{1}H NMR spectrum of compound **4ia** (400 MHz, $CDCl_3$)

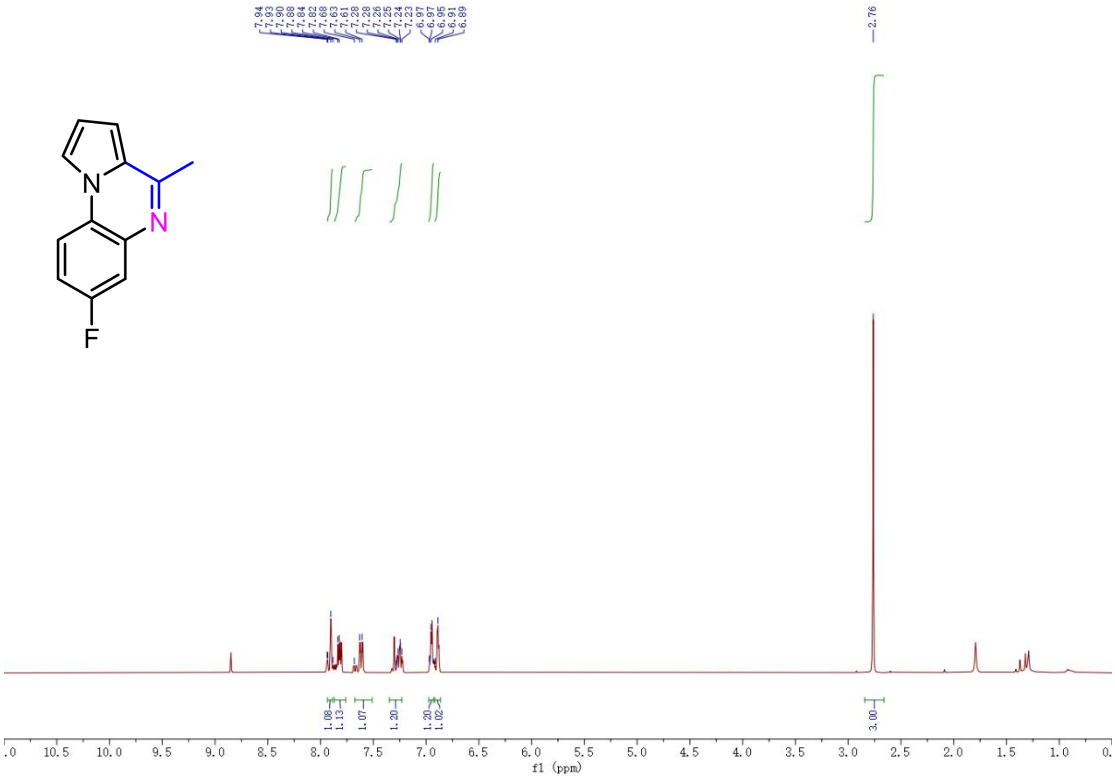

^{13}C NMR spectrum of compound **4ia** (101 MHz, $CDCl_3$)

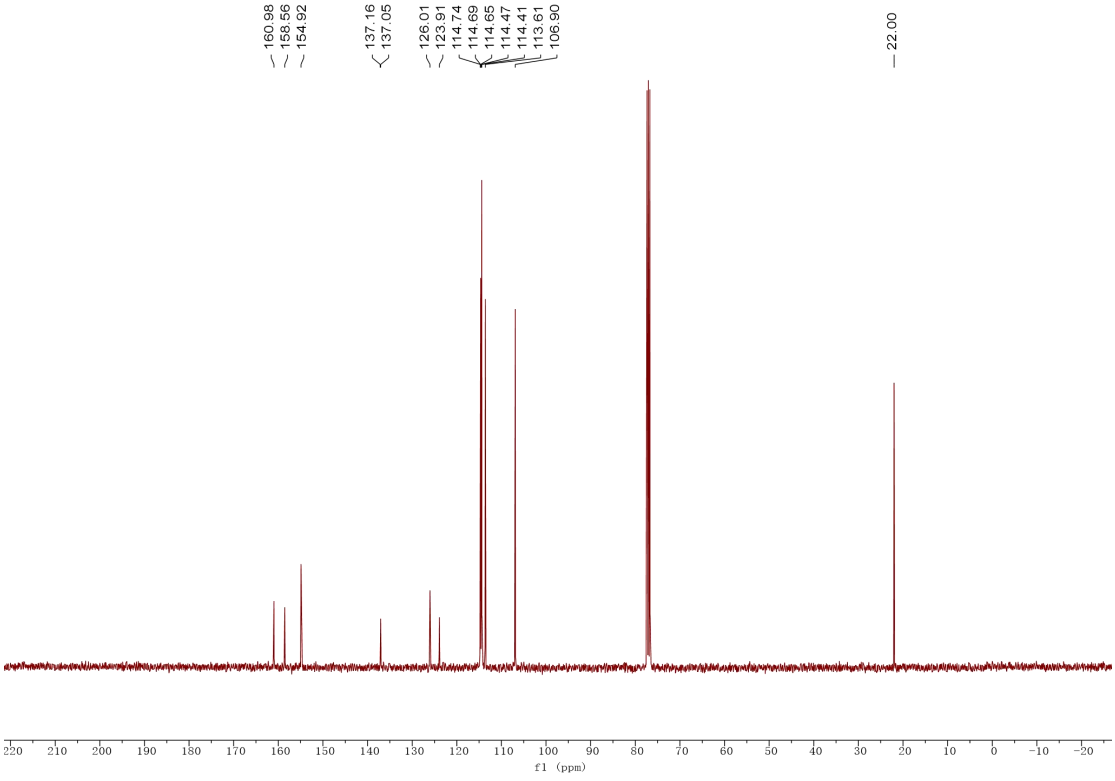

^{1}H NMR spectrum of compound **4ja** (400 MHz, $CDCl_3$)

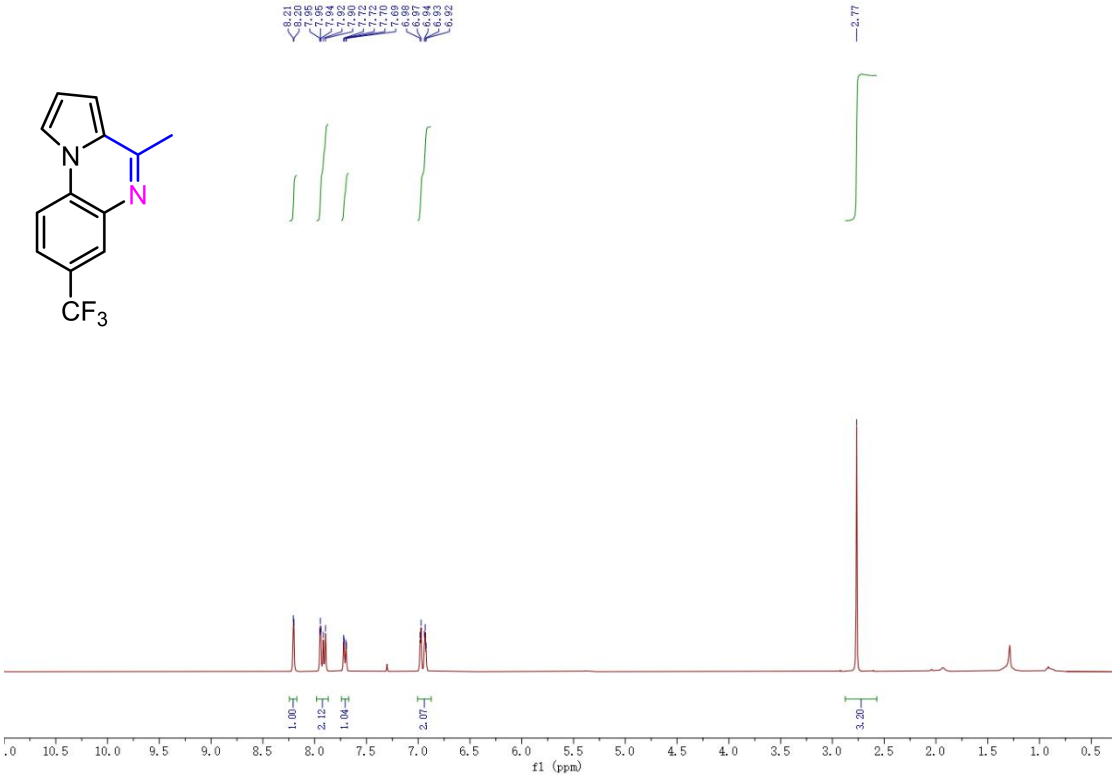

^{13}C NMR spectrum of compound **4ja** (101 MHz, $CDCl_3$)

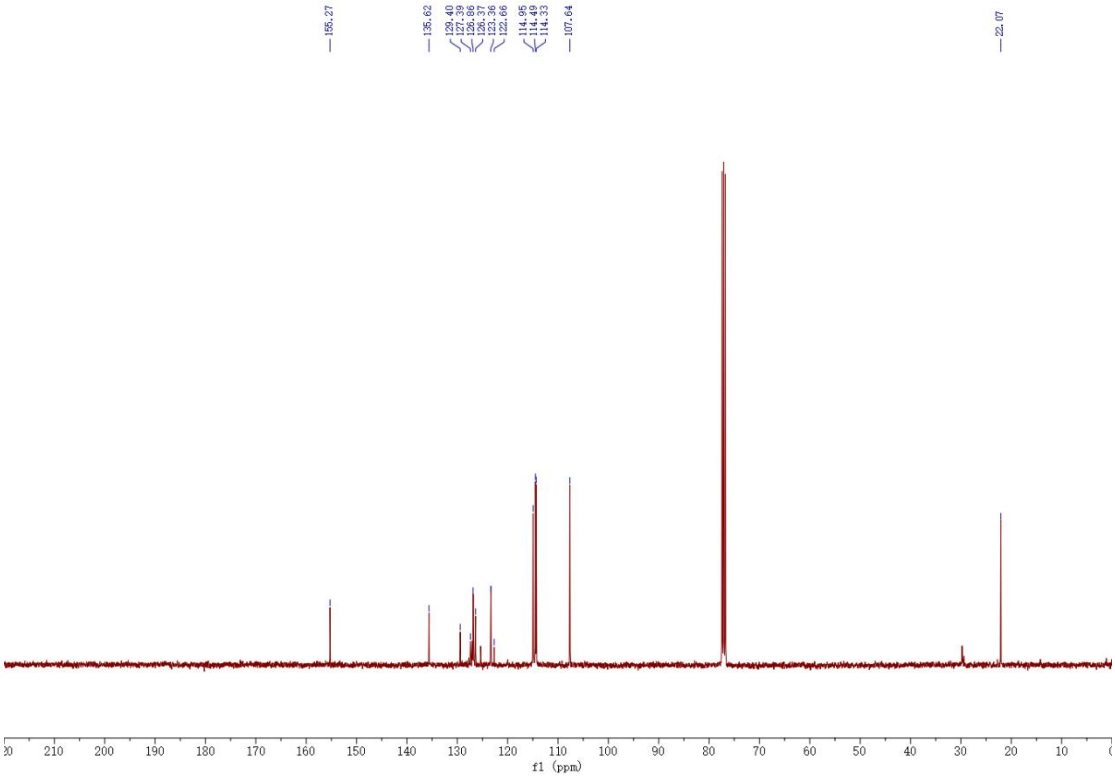

^{1}H NMR spectrum of compound **4ka** (400 MHz, $CDCl_3$)

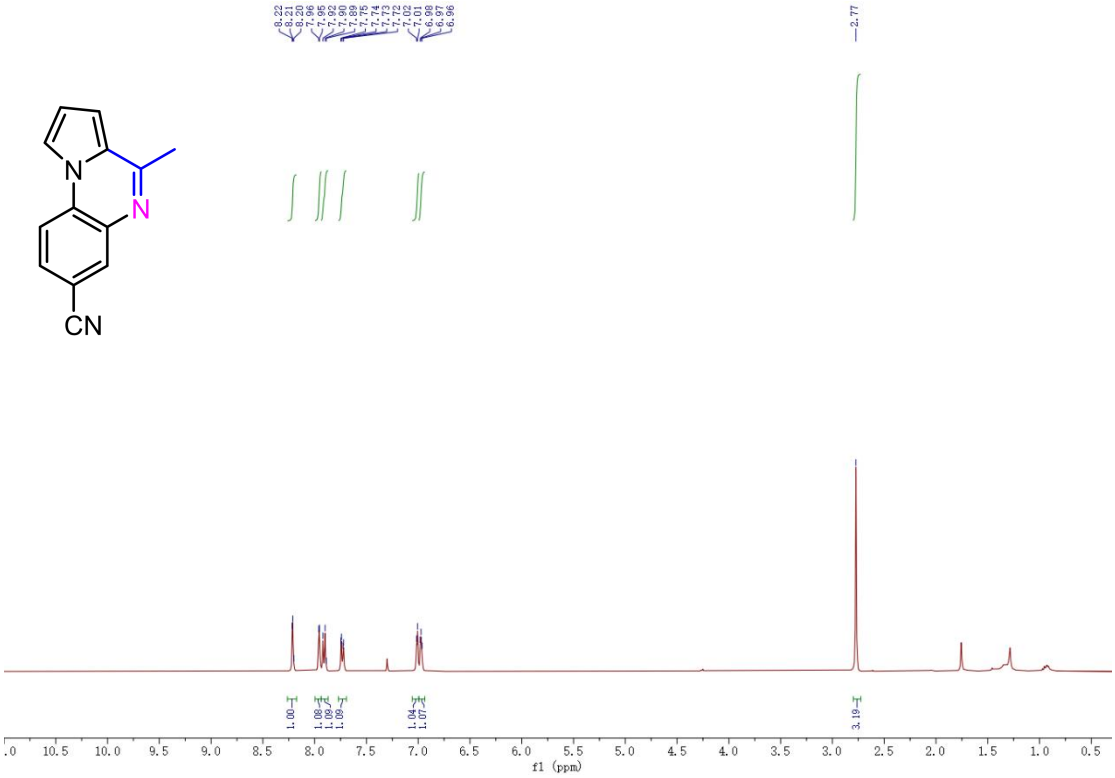

^{13}C NMR spectrum of compound **4ka** (101 MHz, $CDCl_3$)

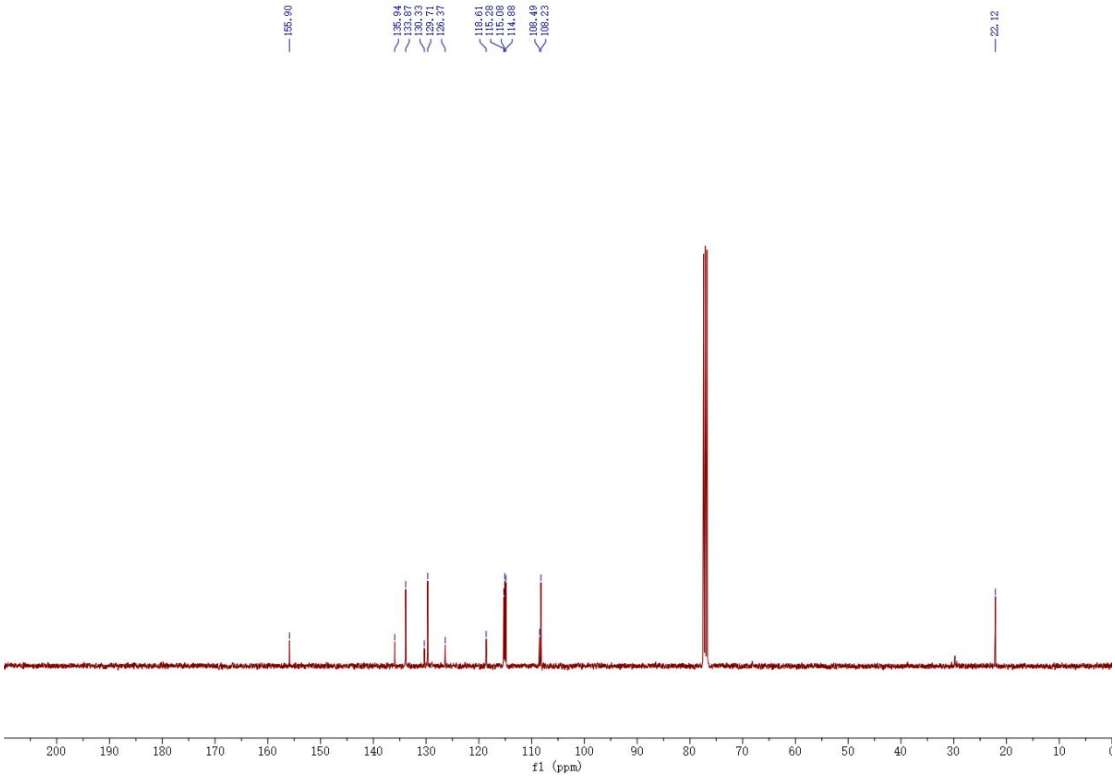

^{1}H NMR spectrum of compound **4la** (400 MHz, $CDCl_3$)

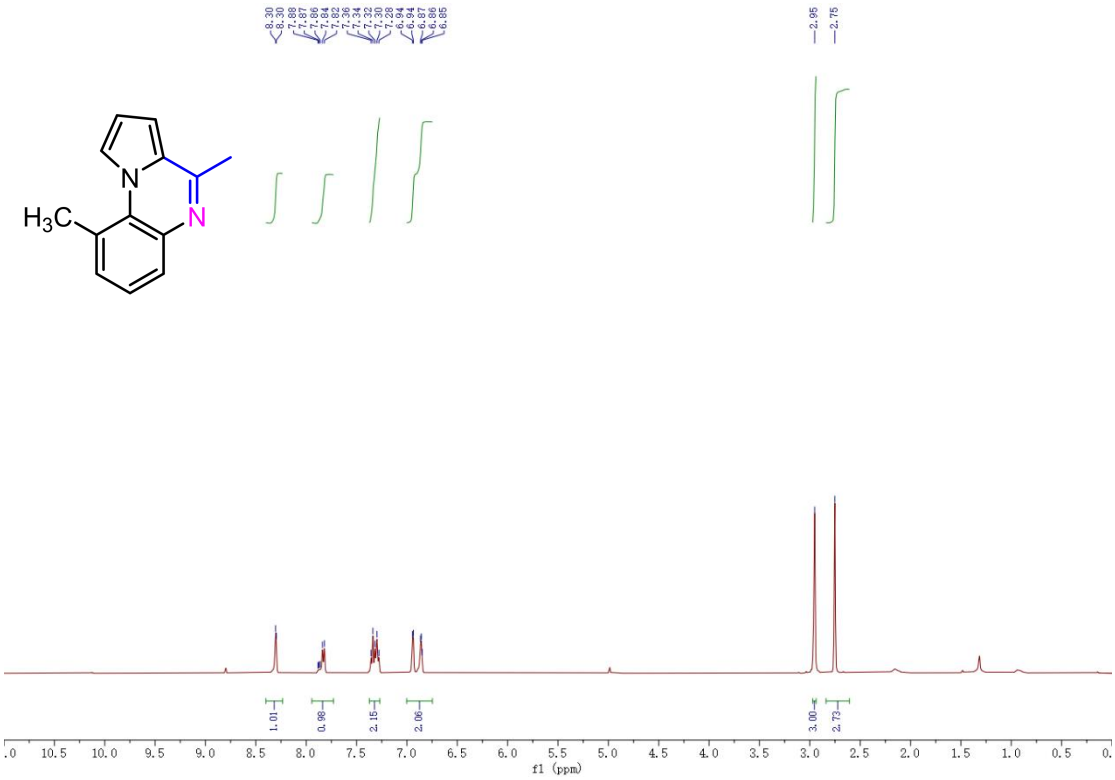

^{13}C NMR spectrum of compound **4la** (101 MHz, $CDCl_3$)

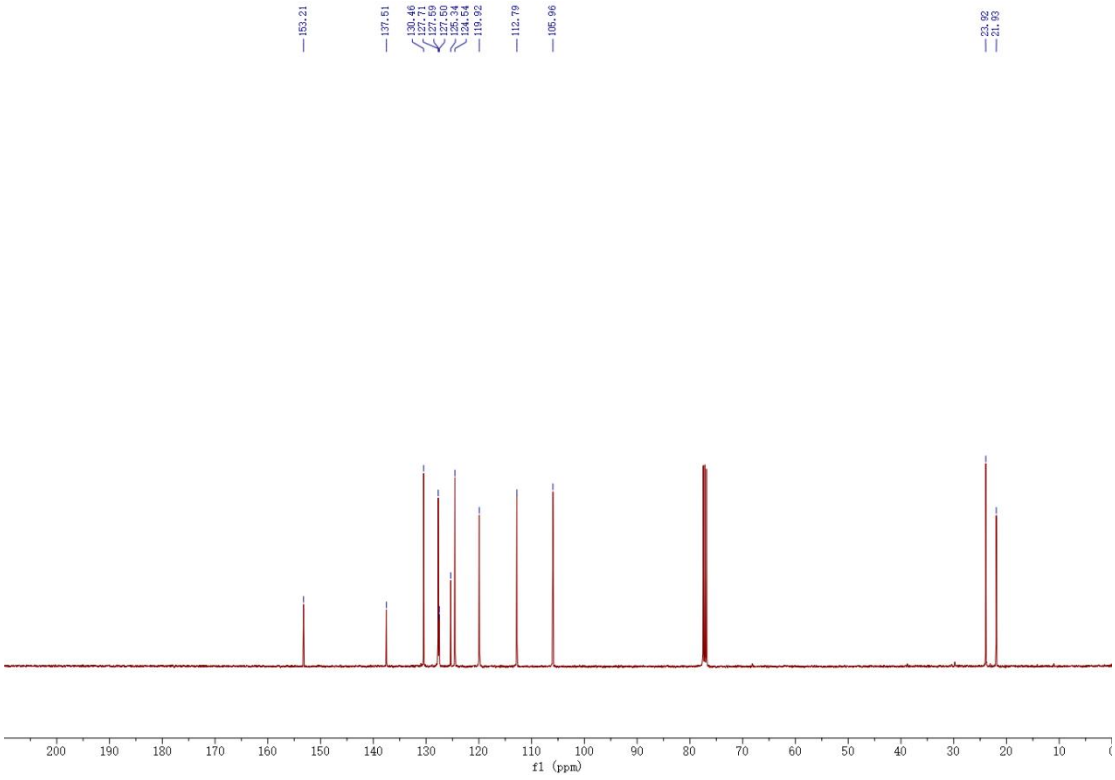

^{1}H NMR spectrum of compound **4ab** (400 MHz, $CDCl_3$)

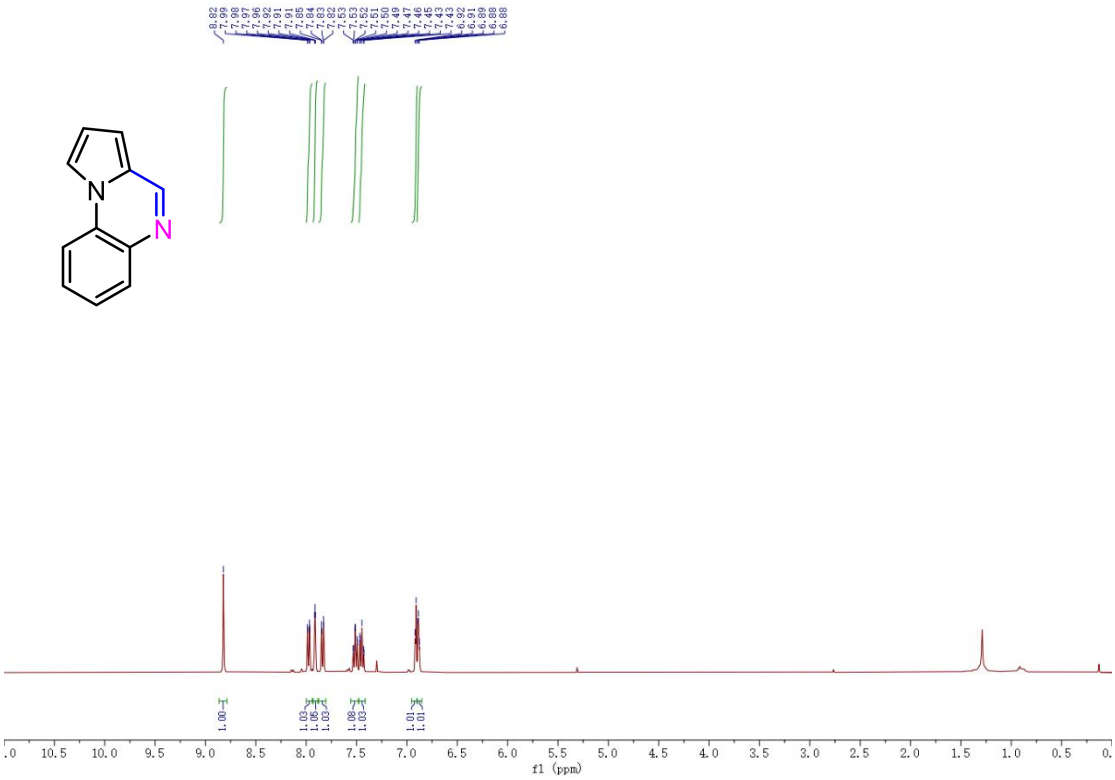

^{13}C NMR spectrum of compound **4ab** (101 MHz, $CDCl_3$)

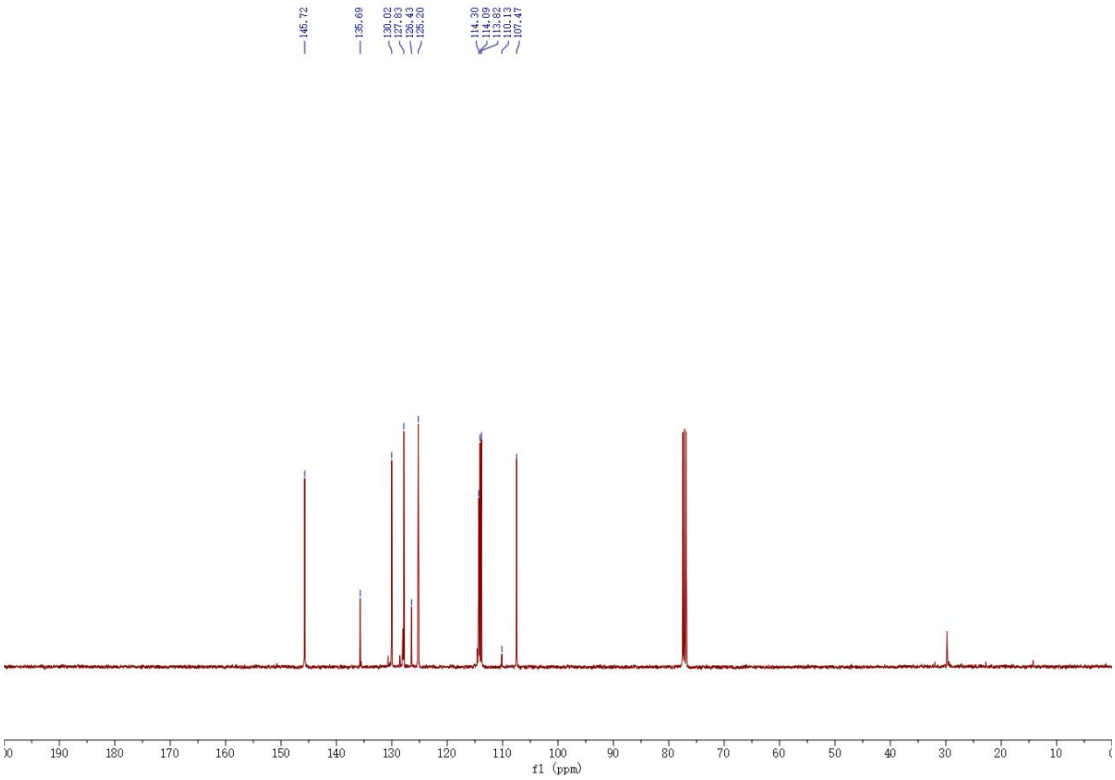

^{1}H NMR spectrum of compound **4ac** (400 MHz, $CDCl_3$)

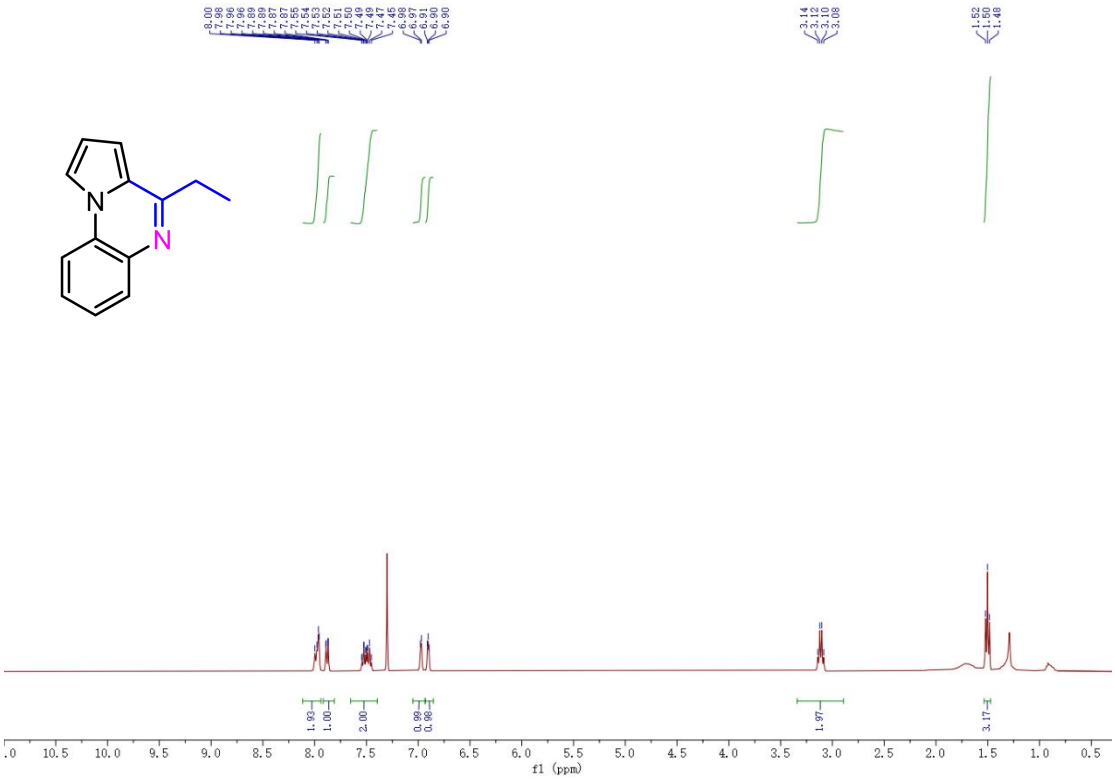

^{13}C NMR spectrum of compound **4ac** (101 MHz, $CDCl_3$)

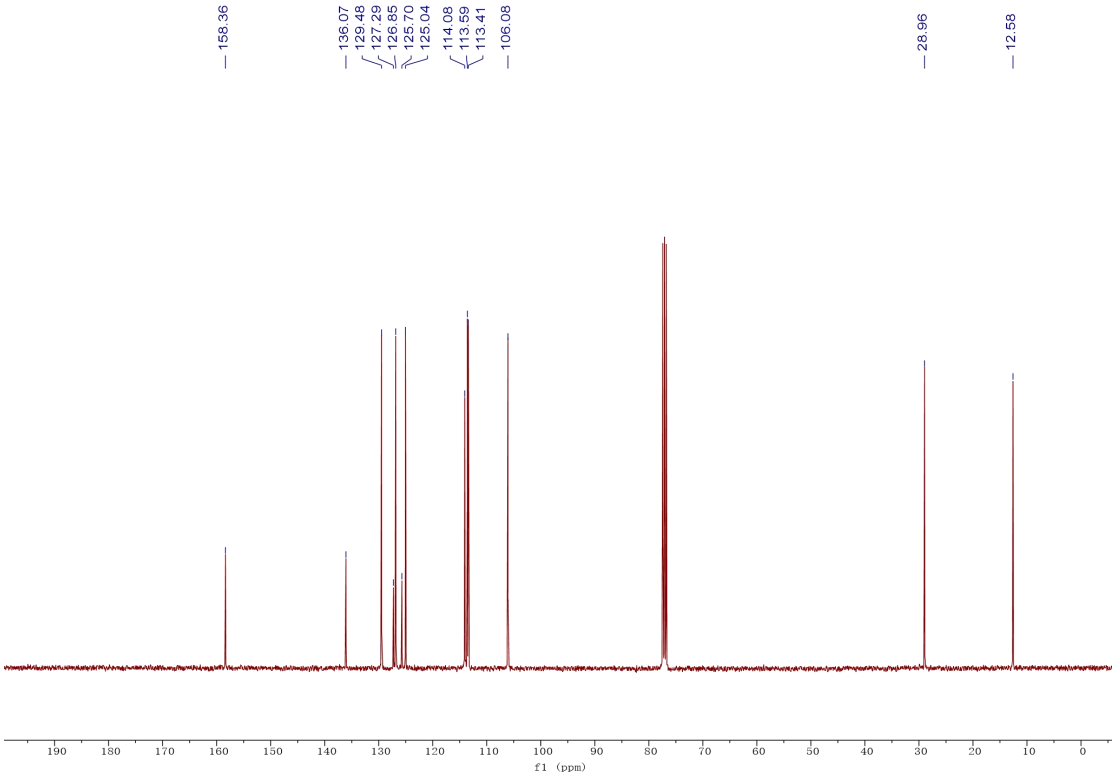

^{1}H NMR spectrum of compound **4ad** (400 MHz, $CDCl_3$)

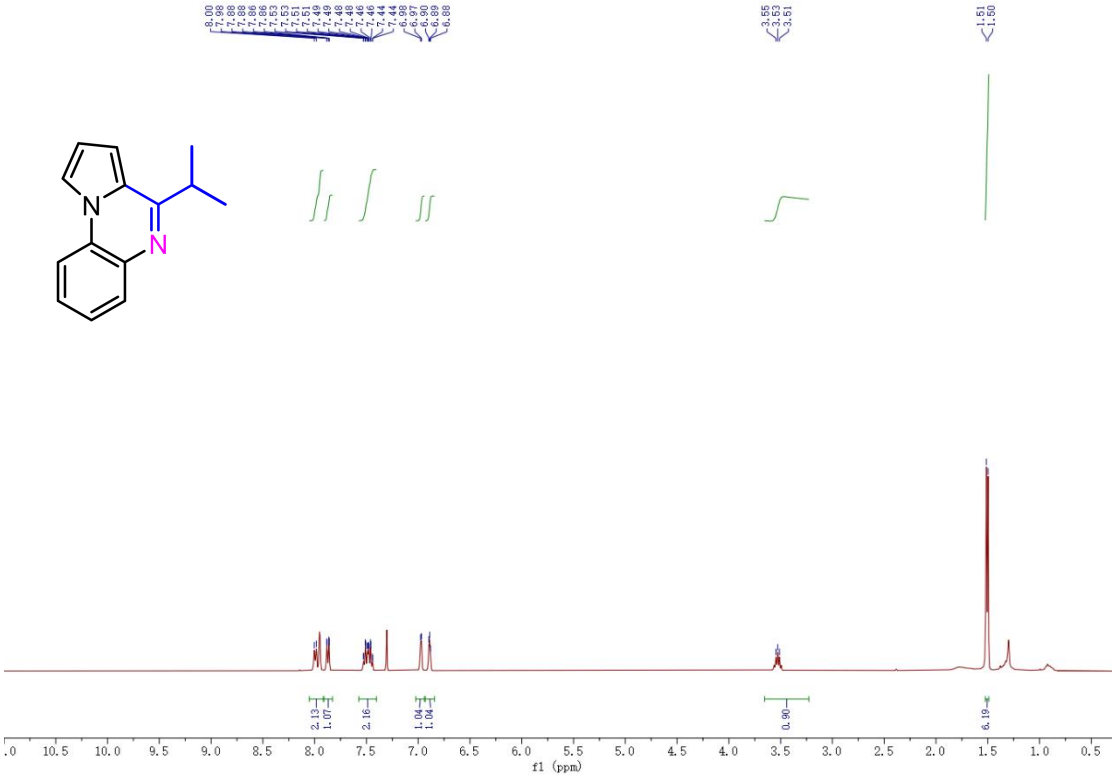

^{13}C NMR spectrum of compound **4ad** (101 MHz, $CDCl_3$)

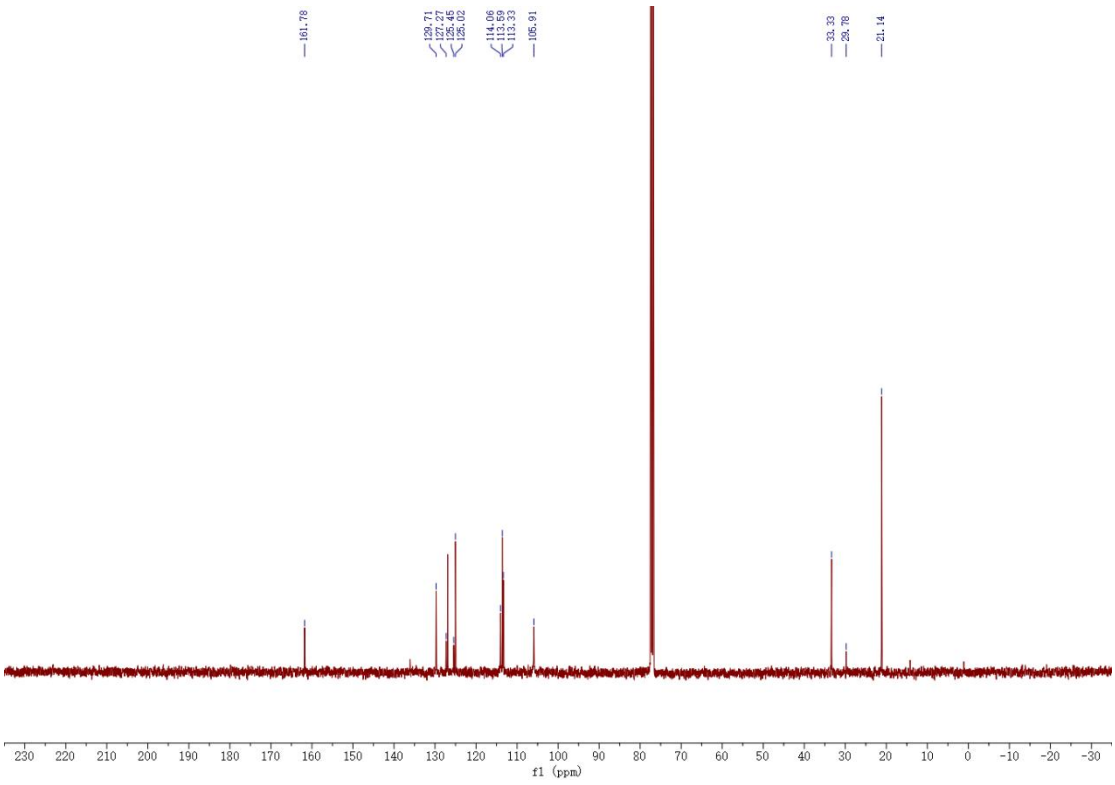

^{1}H NMR spectrum of compound **4ae** (400 MHz, $CDCl_3$)

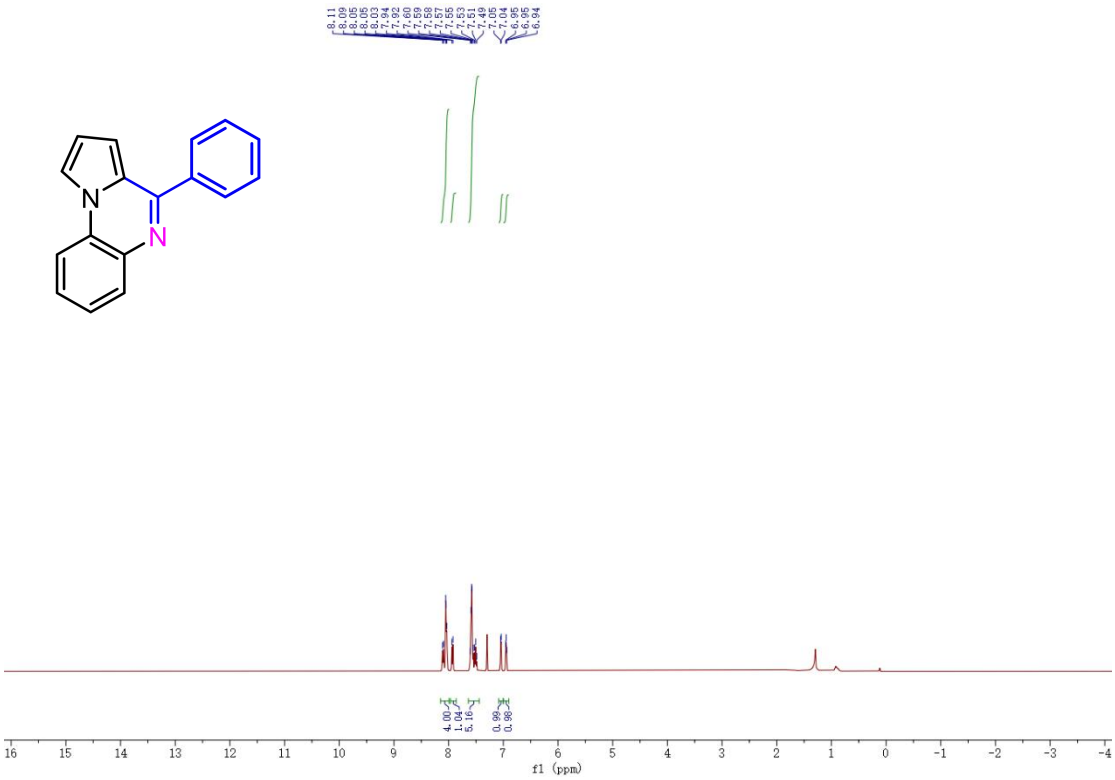

^{13}C NMR spectrum of compound **4ae** (101 MHz, $CDCl_3$)

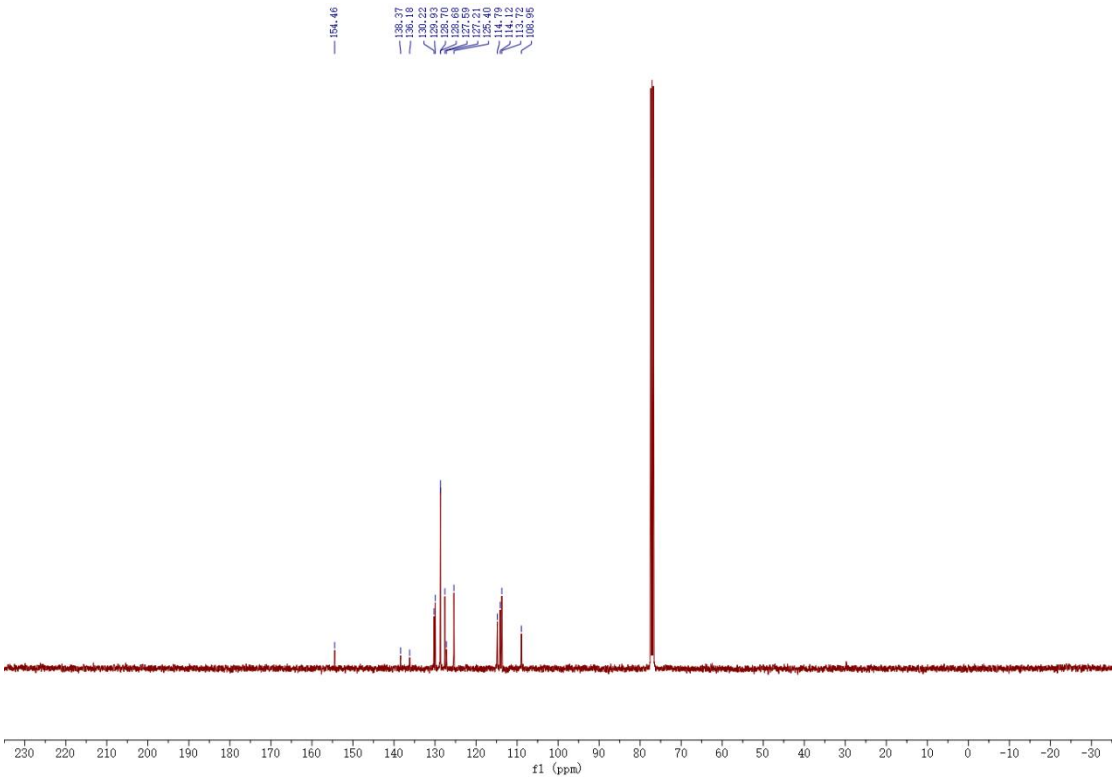

^{1}H NMR spectrum of compound **4af** (400 MHz, $CDCl_3$)

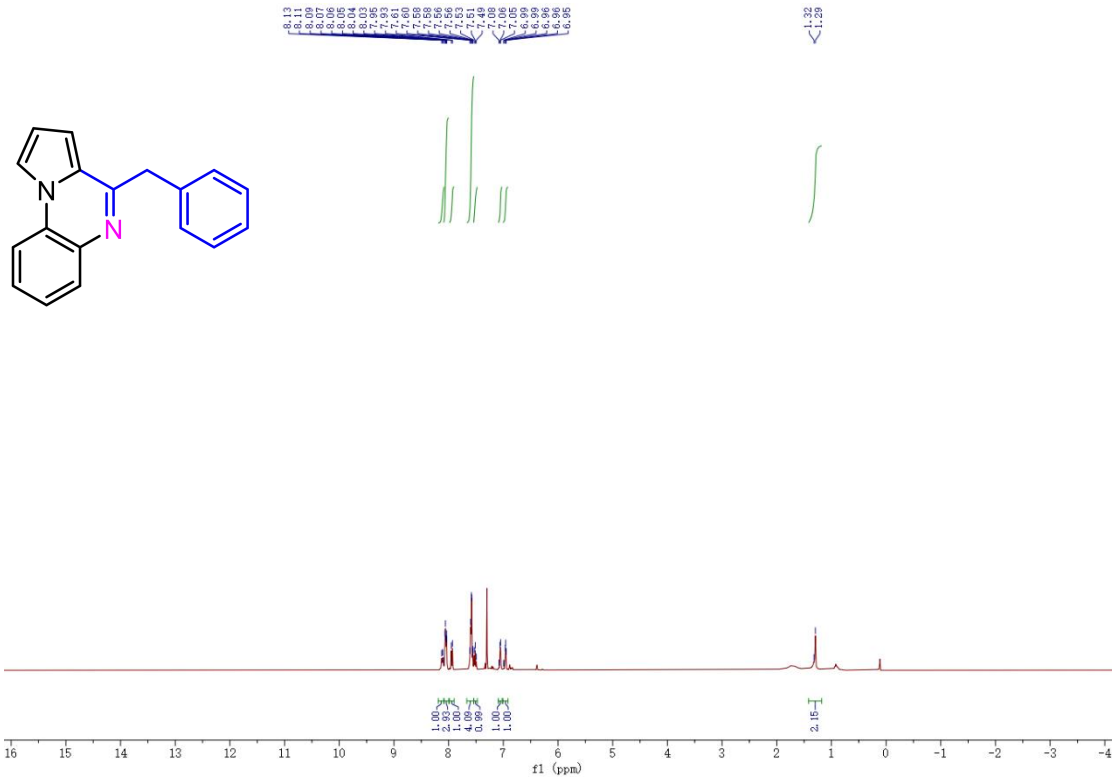

^{13}C NMR spectrum of compound **4af** (101 MHz, $CDCl_3$)

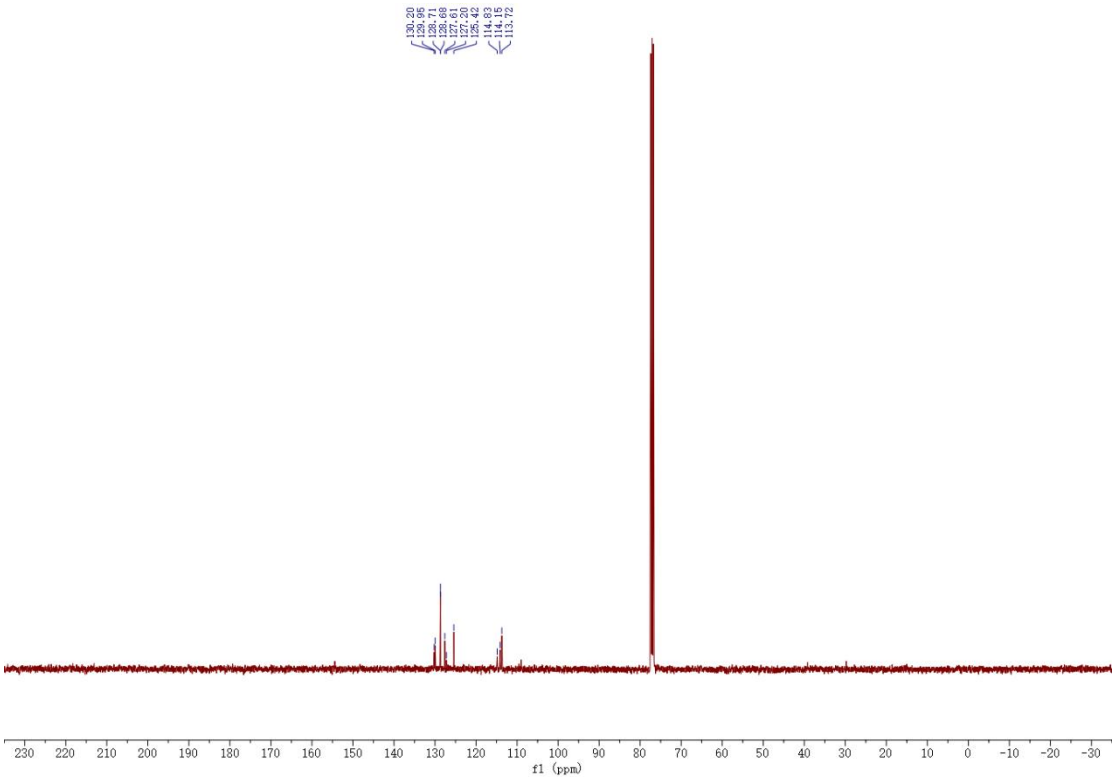

^{1}H NMR spectrum of compound **4ag** (400 MHz, $CDCl_3$)

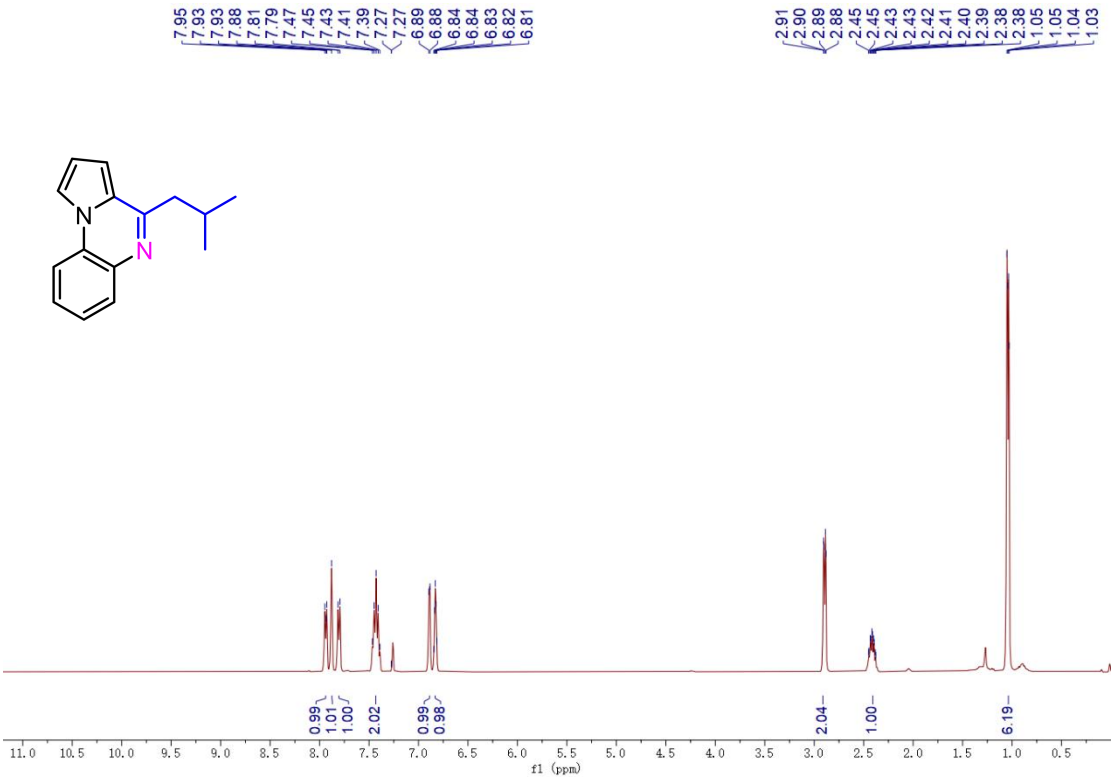

^{13}C NMR spectrum of compound **4ag** (101 MHz, $CDCl_3$)

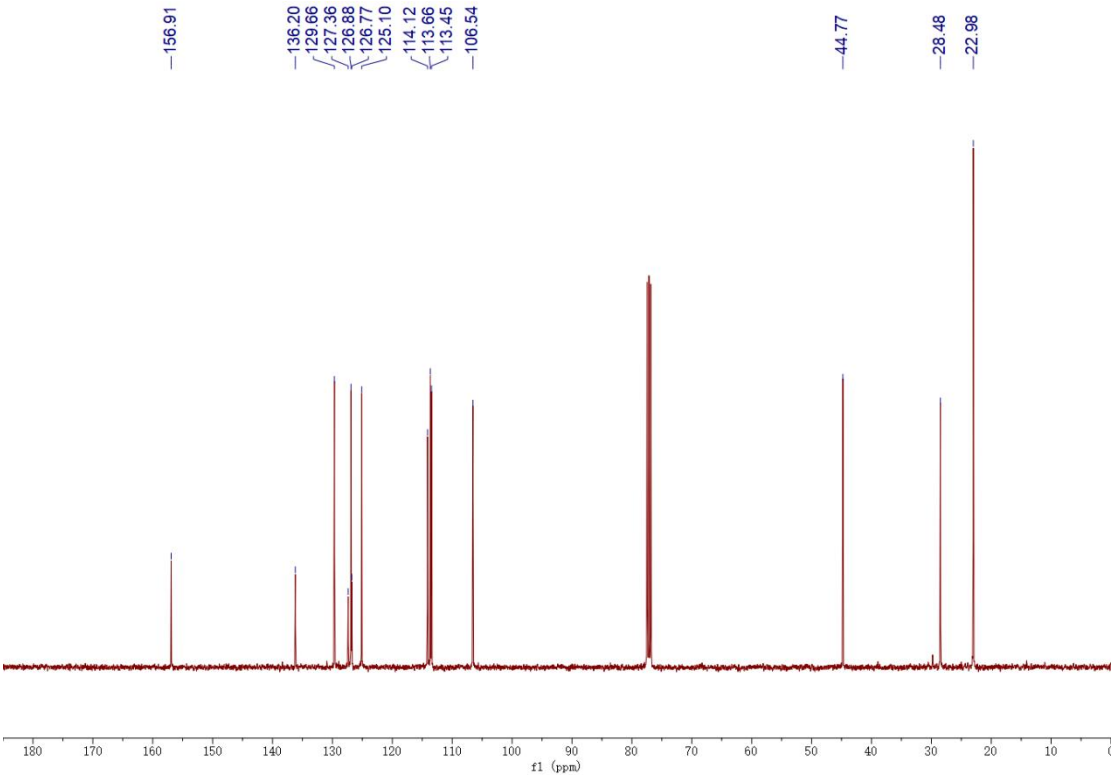

^{1}H NMR spectrum of compound **8** (400 MHz, $CDCl_3$)

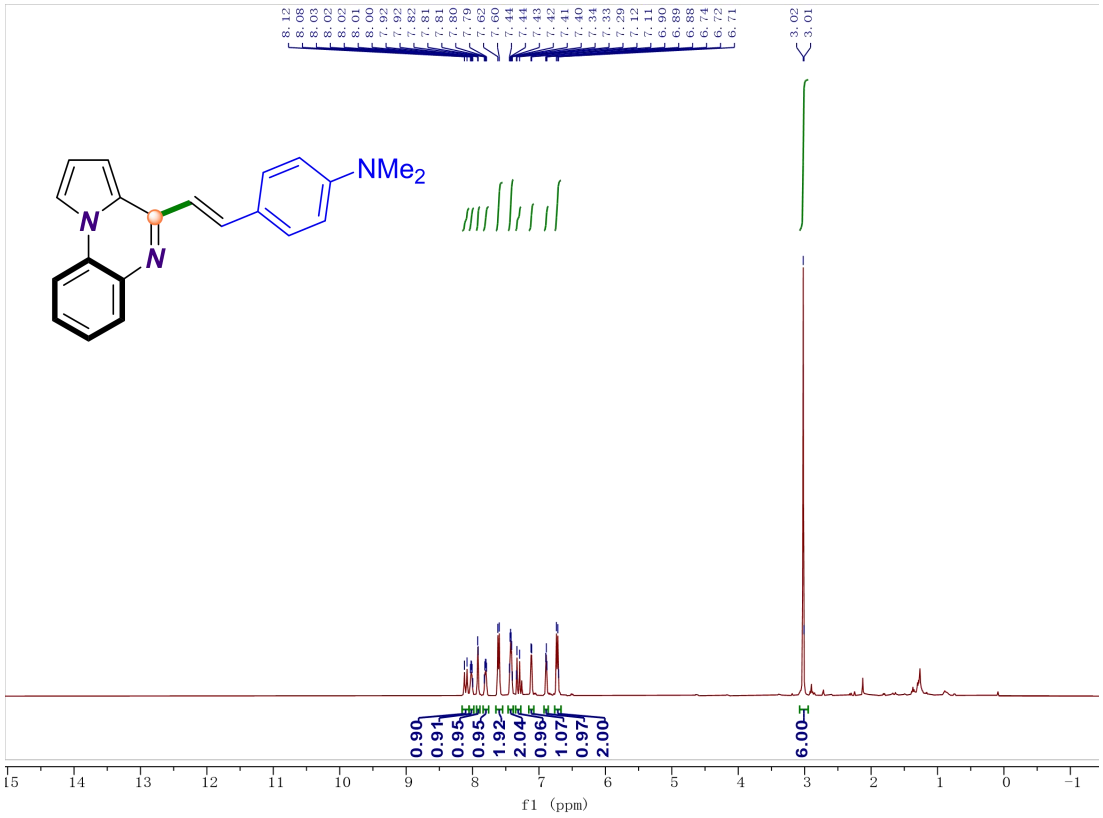

^{13}C NMR spectrum of compound **8** (101 MHz, $CDCl_3$)